ZEOLITE AND HIGH CARBON FLY ASH MIXES AS LINER MATERIALS FOR LEAD/PHENOL SORPTION

GUOBING YUAN

ZEOLITE AND HIGH CARBON FLY ASH MIXES AS LINER MATERIALS FOR LEAD/PHENOL SORPTION

By

© Guobing Yuan, B. Eng.

A Thesis Submitted to the School of Graduate Studies

in Partial Fulfilment of the Requirements for the Degree of

Master of Engineering

Faculty of Engineering & Applied Science

Memorial University of Newfoundland

May, 1997

St. John's, Newfoundland, Canada

ABSTRACT

Two natural zeolites, i.e. chabazite (CHB) and clinoptilolite (CLN), and two coal fly ashes, i.e. Lambton fly ash (LBash) and Nova Scotia fly ash (NSash), were studied toward their suitability as construction materials for landfill liners. Lead (Pb^{2+}) and phenol (C_6H_5OH) were chosen to represent inorganic and organic leachates. The research was focused on (1) the sorption capacity of zeolite and fly ash against Pb^{2+} and phenol; (2) the hydraulic conductivity of these candidate materials when percolated with aqueous solutions of Pb^{2+} (2500 mg/l), phenol (55 mg/l), and Pb^{2+}/phenol mixture (Pb^{2+} = 2500 mg/l and phenol = 55 mg/l), respectively; (3) the interaction among zeolite, fly ash, Pb^{2+}, and phenol; (4) the optimum mix design for zeolite and fly ash in terms of leachate retention and hydraulic performance.

Material characterization revealed that LBash is distinguished from NSash by its unburnt carbon content and surface functional groups. For zeolites, CHB has a higher chemical activity and larger cation exchange capacity than CLN. Batch tests on the four materials demonstrated that CHB was most powerful in Pb^{2+} sorption (210 mg/g) while LBash was most effective in phenol removal (1.3 mg/g). Experimental preference was then given to CHB, LBash, and their mixes.

During column leaching tests, Pb^{2+} sorption took place on LBash and CHB solids through physisorption, chemisorption, complexation, precipitation, and ionic sieving of CHB micro-pores. Phenol was attenuated by LBash and CHB via acid-base reaction, dipole attraction, and hydrogen bonding. In CHB and LBash mixes, CHB was the principal sorbent with Pb^{2+}, while LBash was mainly responsible for phenol retention. When Pb^{2+} and phenol coexist in the system, they compete for all sorption sites except for the CHB micro-pores, which cannot accommodate the size of phenol molecules. The hydraulic conductivity values of CHB and LBash with Pb^{2+} or phenol permeant ranged between 1.7×10^{-8} and 7.0×10^{-8} m/s. Mixes of CHB and LBash are less permeable due to a better filling of pore space. Although the three leachates used as permeant had different chemical properties, they were not concentrated enough to alter the hydraulic conductivity

of test specimens.

It was concluded that, under present experimental conditions, a CHB/LBash ratio of 1:1 in weight appeared to be the optimum mix for a liner material which will exhibit a maximum overall retardation of Pb^{2+} and phenol. The 1:1 mixture compacted under standard condition also showed a minimum hydraulic conductivity in the order of 3.0×10^{-9} m/s.

ACKNOWLEDGEMENT

I gratefully acknowledge the School of Graduate Studies and the Faculty of Engineering & Applied Science at Memorial University of Newfoundland for financially supporting this work.

I wish to convey my sincere thanks to the Fossil Business Unit at Ontario Hydro, SHAW Resources in Nova Scotia, and GSA Resources Inc. in Arizona, USA, for providing fly ash and zeolite free of charge, with very useful technical literature.

I greatly appreciated the technical laboratory support from the Department of Earth Sciences, the Department of Chemistry, and the Department of Biology at Memorial University of Newfoundland.

I would like to thank Mr. Zhiqiang Xu, Mr. Nenyou Jia, and Ms. Li Jin from the Chemistry Department at Memorial University of Newfoundland for sharing their chemistry expertise.

I particularly thank Dr. Pierre Morin for having taken on my supervision, guiding my new venture in the geoenvironmental area, and encouraging me to pursue new career objectives.

I am deeply indebted to my wife, Bingyi, and my daughter, Yixin, for their love and understanding.

TABLE OF CONTENTS

LIST OF FIGURES

LIST OF TABLES

LIST OF SYMBOLS

A	cross-sectional area of a specimen compacted with zeolite and/or fly ash (m^2)
AAS	atomic absorption spectrophotometer
B	Boltzman constant (erg/k)
C, Ci	concentration of Pb^{2+} or phenol measured during a leaching test (ppm)
C_0	initial concentration of Pb^{2+} (2500 ppm) or phenol (55 ppm)
C^*	amount of Pb^{2+}/phenol sorbed per mass of sorbent (mg/g)
C_e	equilibrium Pb^{2+}/phenol concentration in a batch test (ppm)
C_b	equilibrium blank Pb^{2+}/phenol concentration in a batch test (ppm)
CEC	cation exchange capacity (meq/100g)
CHB	natural chabazite
CLN	natural clinoptilolite
D	dielectric constant of the pore liquid in a test specimen
DDL	diffuse double layer
h_i	average head difference between inflow and outflow during Δt_i (m)
IR	infrared radiation
K	hydraulic conductivity (m/s)
K_s	solubility product
L	length of a specimen compacted with zeolite and/or fly ash (m)
LBash	fly ash produced in Lambton generation station, Ontario Hydro

Leachate-1	Pb^{2+} = 2500 ppm
Leachate-2	phenol = 55 ppm
Leachate-3	Pb^{2+} = 2500 ppm and phenol = 55 ppm
LOI	loss on ignition (%)
m	sorbent mass used in a batch test (g)
M	a cation in zeolite formula
M_s	solid mass of a specimen compacted with zeolite and/or fly ash (g)
n	valence of a cation in zeolite formula
n_0	electrolyte concentration of the pore liquid in a test specimen (ions/m^3)
NSash	fly ash from SHAW Resources, Nova Scotia
T	temperature (°K)
T_{pb}	total sorbed Pb^{2+} per gram of specimen solid (mg/g)
Δt_i	time interval between two observations in a leaching test (s)
v_a	valence of cations in the pore liquid of a test specimen
V_i	effluent volume collected during Δt_i (m^3)
SEM	Scanning electron microscopy
$\equiv S$	ash/zeolite solid
V_f	volume of sorbate solution in a batch test (ml)
x	coefficient in zeolite formula
XRD	X-ray diffractometry
XRF	X-ray fluorescence
y	the number of water molecules in zeolite formula

MSW	Municipal solid waste
ZPC	zero point of charge
δ^+ ,δ^-	fractional positive and negative charges on phenol molecules
ε	unit electric charge (Coulomb)
ρ	density of a permeant solution (g/cm^3)
μ	viscosity of a permeant solution ($N \cdot s/m^2$)

1 INTRODUCTION

1.1 The Current Landfilling Practice

1.1.1 Municipal Solid Waste (MSW) and Landfilling

Municipal solid waste (MSW) is generally defined as the combined residential, commercial, institutional, and light industrial solid wastes. In 1989, Canadians generated approximately 1.7 kg of MSW per person per day, which was the highest rate in the world or nearly twice as much as the world average among industrial nations (Hammond, 1991). Of the nation-wide MSW production, more than 80% ends up in Canada's 10,000 landfills; the remainder is incinerated (8%) or recycled (10%) (Government of Canada, 1991). Most existing Canadian landfills are employed as cheap disposal alternatives, far from being state-of-the-art facilities.

In Newfoundland and Labrador, the MSW generation is about 1.4 kg per capita per day, which is mostly disposed in 12 sanitary landfills and 150 other landfill sites (Eaton et al, 1993).

Moreover, according to a survey conducted by the Federation of Canadian Municipalities in 1990, "landfills serving 22% of the Canadian population will be full within two years. By 1995, existing landfills serving 71% of the population will be full" (Government of Canada, 1991). Many communities in this country have a critical need for new landfill space or new alternative solutions.

1.1.2 High Performance Landfill Liner

Landfills release leachate as a consequence of external moisture inputs and internal

soluble waste constituents. The release, if uncontrolled, eventually reaches surface water and groundwater, posing potential threat to the environment and human health. Cases of leachate contamination have been repetitively reported, ranging from slight degradation of water quality to the presence of toxic heavy metals and organic compounds (Moell 1977, USEPA 1977, and Cyr et al 1987). Cleaning up of a contaminated site needs, however, a long and expensive action.

To protect the public from potential environmental risk, modern engineered landfills should include "impermeable" upper covers and bottom liners, augmented by sufficient drainage and venting to handle the detrimental leachate and gas emission. The most critical part in a landfill system is perhaps the bottom liner, which works as a barrier to limit leachate movement, and retain different contaminants. In particular, the development of liner technology is of immediate importance when many old Canadian landfills are approaching closure and new landfill sites are being considered.

Furthermore, changes that can be anticipated in the nature of future landfills should also be taken into account in liner design. In 1989, the Canadian Council of Resource and Environment Ministers (now the Canadian Council of Ministers of the Environment) set an ambitious goal of a 50% reduction in solid waste over 1988 level by the year 2000. The implementation of 4Rs (i.e. Reduction, Reuse, Recycling, and Recovery) strategy should substantially reduce the disposal of non-hazardous degradable wastes. The waste stream going to the post-2000 landfills will mainly contain non-degradable hazardous substances, such as MSW incineration ash and leachate treatment residues. Leachate from such harsh landfill sites will be far more concentrated than that

detected from today's facilities in terms of certain chemical indexes, e.g. heavy metal ions (Hwa 1991). Not all liner materials proposed so far, including compacted admixture of soil/sand and clay, and geosynthetics, can tackle the challenge of concentrated leachate for a specific service time.

Therefore, it is very desirable to propose **high performance liner materials** that are capable of **(1) effective reduction of leachate leakage,** and **(2) safe containment of organic and inorganic leachate contaminants during a long-term lifespan.**

To achieve these two goals, a composite liner is usually preferred to a simple liner constructed with a single material. Composite liners are made of dissimilar materials, such as admix of soil/sand and cohesive clay like bentonite, sandwiched between two geomembranes. Figure 1.1 is an example composite liner unit.

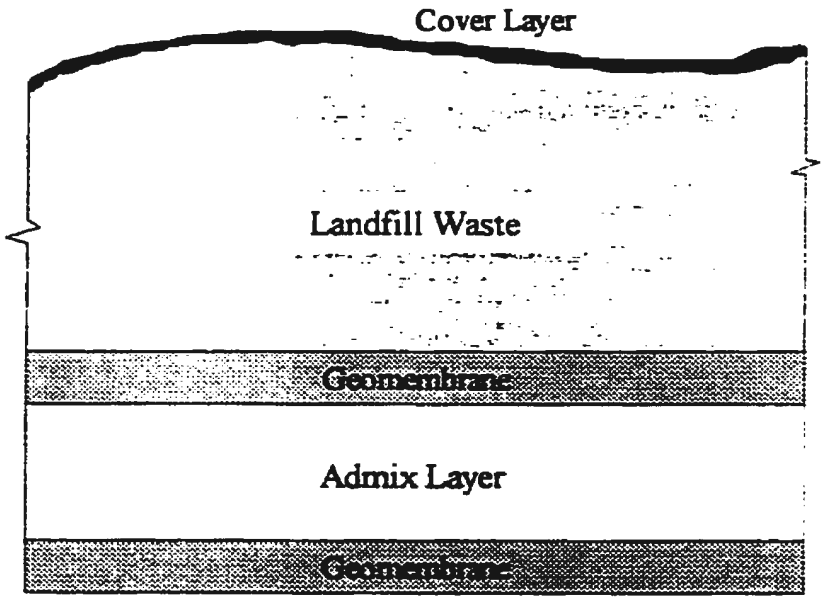

Figure 1.1 A composite liner unit

As far as contaminant sorption and capital cost are concerned, **natural zeolite** and **high-carbon fly ash** are among the most promising admix materials. Zeolite is a common aluminosilicate mineral distributed worldwide in sedimentary deposits. The environmental importance of zeolite has been recognized in pollutant containment due to its excellent features of ion-exchange, sorption, and sieve-like selectivity. Natural zeolite is remarkable in heavy metal decontamination against various waste streams including MSW leachate. As for coal fly ash, it is a waste by-product from coal-fired power stations. The increasing difficulty of ash disposal makes it desirable to reuse fly ash in any potential engineering area. An innovative utilization of fly ash in landfill liner construction has been extensively attempted. Fly ash with high carbon content is especially useful in adsorbing organic contaminants from landfill leachate. Therefore, it is expected that combination of high carbon fly ash and natural zeolite will give rise to an unbiased retention of organic and inorganic species from real leachate. Since natural zeolite and fly ash are both cheap materials with main costs being transportation, their mixture will also be commercially competitive.

1.2 The Objective of This Study

The complexity of composite liners requires integrated knowledge of several disciplines. Clay mineralogy gives an insight into the basic structure of soils/clays that helps understand the interaction of these solids with water and leachate chemicals. Environmental toxicities of various leachate contaminants need to be identified, so that a liner can be designed to focus on specific species of environmental concern. Chemical

mechanisms, such as hydrolysis, adsorption, ion exchange, complexation, and precipitation, are key factors that control the sorption behaviour of liner materials, and the compatibility of the chosen materials with the leachate at hand. Also, hydraulic and mechanical properties deserve equal consideration in order to prevent liner failure due to high hydraulic conductivity and poor material strength.

The present study will deal with the above-stated aspects for an admix layer consisting of zeolite and high-carbon fly ash. Five objectives are aimed at here through laboratory investigation:

(1) identify active zeolite and high-carbon fly ash from candidate materials. The former should possess high selectivity for heavy metal adsorption. The latter is expected to show special affinity to organic compounds;

(2) Evaluate the sorption potential of zeolite and high-carbon fly ash with concentrated organic and inorganic leachates, represented by synthetic Pb^{2+} and phenol solutions;

(3) probe the interactions between the sorbents and leachate chemicals so as to determine the chemical compatibility of the liner materials with leachate of interest;

(4) Assess the hydraulic compatibility of the compacted mix of zeolite and fly ash;

(5) propose an optimum mix of zeolite and carbon-rich fly ash in terms of its overall sorption and resulting hydraulic conductivity.

1.3 Organization of the Thesis

The thesis consists of 7 chapters, the contents of which are as follows:

Chapter 1 - Introduction: the current landfilling practice and the significance of a composite liner.

Chapter 2 - A review of preceding generations of landfill liners, zeolite and fly ash as new materials for liner construction.

Chapter 3 - Materials and their characterization.

Chapter 4 - Description of the experimental methods used.

Chapter 5 - Presentation of experimental results, i.e. sorption isotherms of the test materials with lead (Pb^{2+}) and phenol, hydraulic conductivity measurements, and Pb^{2+}/phenol breakthrough curves from leaching tests.

Chapter 6 - Interpretation of the results, i.e. the effects of zeolite/fly ash hydration and permeant chemistry on hydraulic conductivities, mechanisms of Pb^{2+} sorption, mechanisms of phenol sorption, impact of phenol on Pb^{2+} sorption, partition of Pb^{2+} among different sorption sites, and the relationship between the sorption efficiency and the zeolite-to-fly ash ratio.

Chapter 7 - Conclusion about the optimum zeolite/fly ash mixture.

2 LITERATURE REVIEW

2.1 Preceding Generations of Liner Materials

Typical liner materials are summarized in Table 2.1.

Table 2.1 Liner materials (Folkes, 1982)

Type	Typical material	K (m/s)
Compacted clayey soil	Local clayey soil	10^{-8} to 10^{-10}
Admixes	Bentonite-sand	10^{-8} to 10^{-10}
	Soil cement	10^{-10} to 10^{-11} (lab) 10^{-8} to 10^{-9} (field)
	Soil asphalt	
Geo-membranes		10^{-11} to 10^{-14}
	(1) Thermoplastics Polyvinyl chloride (PVC) (2) Vulcanized elastomers Butyl rubber (3) Crystalline thermoplastics Low density polyethylene High density polyethylene	
Spray-ons	Asphalt	10^{-9} to 10^{-11}
Sealants	Polyacrylamide	
Sorbents	Silica-alumina Clays Textile fibers	

The hydraulic conductivity of a compacted clay mainly depends on its grain and pore size distribution, and particle and aggregate orientation. Given a specific clayey material, compaction water content shows a very significant effect on clay permeability. Compaction at a water content that is less than optimum water content results in a structure composed of shear-resistant aggregates and relatively large, continuous macropores. Compaction at a water content that is greater than optimum water content results in shear deformation of the aggregates, and reduced macropores. As a result, a clay compacted dry of optimum will be 2~3 orders of magnitude more permeable than that compacted wet of optimum, when both are saturated with water during the measurement of hydraulic conductivity (K, m/s) (Mitchell et al, 1965). If fine-grained local soil is available, it will be an economic option for liner construction. However, naturally occurring clayey soil is somewhat heterogeneous in nature, silt or sand lenses may impair the integrity of the compacted liner. In addition, the local soil usually only has a limited capacity to withdraw chemicals from leachate. Once the capacity is exceeded, the chemicals are likely to escape from the liner.

Admixed liner materials include bentonite-sand mix, soil cement, and soil asphalt. Low permeability of bentonite-sand mix can be ensured by bentonite additive, which has a relatively high cation exchange capacity (CEC), i.e. ~70 meq/100g, but very low organic carbon content. The mixture cannot provide adequate attenuation for both inorganic and organic contaminants present in concentrated leachate. Compacted asphalt mixture and soil cement have laboratory K values of as low as $10^{-10} \sim 10^{-11}$ m/s (Matrecon Inc, 1980), but field K values are generally much higher.

Geomembranes are polymeric synthetics, such as thermoplastics, vulcanized elastomers, and crystalline thermoplastics. Typical geomembranes are 4~8-mm-thick flexible sheets, which can be bonded to adjacent sheets with thermal or chemical bonding equipment. Presumably, geomembranes are voidless continuums that completely prevent leachate leakage. However, even a brand-new, delicately installed liner of high density polyethylene (HDPE, the preferred polymer for liners) still cannot totally prevent leakage due to pinholes and failed seams. Besides, HDPE allows some organic chemicals to diffuse through it quite readily (Rowe et al 1996, and LaGrega et al 1994).

Spray-ons like emulsified asphalt and liquid vinyl polymer were reported to have laboratory K values of less than 10^{-11} m/s. Field K values are higher because of pinhole and uneven coverage. Polyacrylamide sealants, if mixed in situ, may result in relatively high seepage rates.

Sorbent materials include oxides (e.g. alumina-silica), clays, and textile fibers. They are important constituents or potential analogs of soils. Contaminants are sorbed onto negatively charged sorbent materials due to a combination of electrostatic, hydrophobic, ion exchange, and/or other specific chemical interactions. Zeolite and coal fly ash, both being alumina-silica, belong to the sorbent category. Because of their open structure and extraordinarily high CEC value, zeolites are superior to other geosorbents in retaining inorganic ions. Coal fly ash, if rich in carbon content, can strongly sorb organic compounds in a similar manner to activated carbon.

2.2 Zeolite and Fly Ash

2.2.1 Fly Ash: A Waste By-product

Coal ash is a waste by-product generated by pulverized-coal-fired power stations. The ash predominantly results from non-combustible constituents present in coal such as minerals formed during geologic deposition of the coal. Coal ash is generally composed of 15% bottom ash and 85% fly ash. The bottom ash is a slag-like material formed at the bottom of station boilers. The fly ash is a fine powdery material collected typically by electrostatic precipitators.

Fly ash is inherently a mixture of spherical particles, crystalline matter and unburned carbon. Ashes vary in nature from plant to plant with the type of coal being used, the method of firing, and the way in which the ash is collected. Fly ash contains a large quantity of silica (SiO_2), alumina (Al_2O_3), ferric oxide (Fe_2O_3), and smaller quantity of other oxides such as CaO, MgO, K_2O, Na_2O, SO_3, and P_2O_5. The carbon content is reflected in the loss on ignition (LOI), ranging between 0.1~12.0%. However, high-carbon fly ash may contain unburned carbon up to 15% (Heystee et al, 1991). Although it has water soluble contents, fly ash is exempted from "hazardous" classification (Heystee et al, 1991).

A typical 500-MW power plant, in a 35-year service life time, would need at least 160 ha of land to dispose 4 Mt of its total ash yield to a 3m height (Wright, 1980). Based on 1989's share of coal burning electricity generation (approximately 17,500 MW, Government of Canada, 1991), the disposal of total annual ash production in the country requires 160 ha of land piled to 3m. The land consumption due to fly ash accumulation

is growing from year to year. Owing to public opposition and regulatory restriction, disposal of fly ash, even as a nontoxic material, becomes increasingly difficult. This logically calls for fly ash utilization in different engineering sectors. The pozzolanic property makes fly ash a beneficial ingredient in cement industry. Cement so modified improves concrete strength and durability (Berry, 1978). Fly ash also found its commercial market in land reclamation, brick production, road construction, mine backfilling and hazardous waste stabilization (Chan, 1990).

2.2.2 Fly Ash for Liner Use

Innovative utilizations of fly ash in landfill liner design were reported by different investigators. Vesperman et al (1985) appear to be the first authors to evaluate the potential of fly ash for liner use. Tests on hydraulic conductivity were performed on fly ash mixed with quartz sand. The addition of pozzolanic fly ash to permeable sand produced 10^3 to 10^4 fold permeability reduction with final hydraulic conductivities of less than 10^{-9} m/s.

Bowders (1988) proposed stabilized fly ash as liner material for waste disposal facilities. Hydraulic conductivities around 10^{-8} m/s were obtained when 15% of lime or cement was added to the ash. Much lower values (10^{-10} m/s) were obtained by substituting bentonite for the lime or cement. The addition of lime or cement stabilized the fly ash with respect to toxic leachate elements, but bentonite was not found successful at fixing the elements onto the particular fly ash.

Similar fly ash admixes were suggested by Chan (1991), Edil et al (1992), and

Nhan (1994). The laboratory permeants used were mostly distilled water or inorganic solution. Further investigation on fly ash using organic permeant in conjunction with inorganic leachate is therefore deemed necessary.

2.2.3 Zeolite: A Distinguished Mineral

Zeolites are crystalline aluminosilicate minerals which include nearly 50 natural species and more than 100 synthetic species. The empirical formula for a zeolite mineral is

$$M_{2/n}O \cdot Al_2O_3 \cdot xSiO_2 \cdot yH_2O$$

where *M* is Na, Ca, K, or another alkali or alkaline earth cation; *n* is the valence of that cation; *x* is a number equal to or greater than 2; *y* is the number of water molecules that indicates the pore volume; and $x/2+1<y<x+2$. Structurally, the fundamental building block in the "framework" aluminosilicates is the $(Al, Si)O_4$ tetrahedron. Each of the four oxygen anions is shared with another tetrahedron to extend the crystal structure in three dimensions. The resulting crystal is unusual in that it is honeycombed with relatively large cavities. The water of hydration is contained within these cavities. The intracrystalline voids that are available for sorption make up to 30 to 50% of the total crystal volume of major zeolites (Mumpton, 1984). Ions can migrate rather freely through the open structure, some cations fitting more snugly in the cavities than others. Consequently, zeolites act as cation exchangers. In addition, zeolites may behave as molecular sieves if the water adsorbed in cavities is completely or partly removed. Uncharged molecules, like organic compounds, can be selectively sorbed depending on

their sizes.

Because of their unique properties of ion exchange and selective sorption, zeolites have gained increasing application in numerous scientific and technological areas. "Rarely in our technological society does the discovery of a new class of inorganic materials result in such a wide scientific interest and kaleidoscopic development of applications as has happened with the zeolite molecular sieves" (Breck, 1974).

With regard to geological occurrence and commercial significance, clinoptilolite, mordenite, phillipsite, chabazite, and erionite are the five most important species of natural zeolite. Nearly 2000 sedimentary occurrences have become known of sufficiently large tonnage and high purity in more than forty countries (Mumpton, 1984).

2.2.4 Zeolites in Environmental Technology

Both the ion-exchange and sorption properties of natural zeolites have been well recognized in the field of pollution remediation, including radioactive waste disposal, sewage effluent treatment, treatment of mining and hydrometallurgical effluent, and control of solid and hazardous wastes.

The specificities of clinoptilolite and chabazite for the removal of radioactive wastes were announced by Ames (1960) and Mercer et al (1970a). After radioactive solutions passed through zeolite columns, cesium and stronium ions were extracted with high efficiency from waste streams. Natural zeolites are not only less expensive than organic ion-exchange resins, they are also much more resistant to nuclear degradation. This is an important attribute to the safe development of the nuclear power industry.

For sewage effluent treatment, zeolites were suggested to remove ammonia nitrogen, which may otherwise cause rapid growth of algae and lead to eutrophication of lakes and steams. Clinoptilolite and chabazite have special preference for NH_4^+ adsorption. Ion-exchange process using clinoptilolite can remove up to 99% of the contained ammonium ions from tertiary sewage effluent (Mercer et al, 1970b).

Another significant use of natural zeolites is to remove heavy metals from wastewater effluents of mining and metallurgical operations. Although the removal efficiency is dependent of the selectivities of individual zeolites for heavy metal ions, zeolites can contribute heavily towards eliminating a large part of the heavy metal content in industrial wastewater.

As silicates, natural zeolites also react readily with clay or cement so as to solidify and stabilize hazardous wastes in final solid matrix. This idea can be applied in designing landfill liner. According to Evans et al (1990), composite liner materials of chabazite and silty clay preferentially adsorb heavy metals as compared to the pure silty clay, and lead is more likely to be adsorbed than is copper. Although little can be seen in the literature on this topic, competitive usefulness of zeolites can be foreseen for the design of high performance liners.

3 MATERIALS AND SYNTHETIC LEACHATE

3.1 Fly Ash

Two candidate coal fly ashes were characterized for preliminary study. One is LBash that is produced in Lambton generation station, Ontario Hydro; another is NSash supplied by SHAW Resources, Nova Scotia. Both are fine powdery materials, with more than 80% passing the #200 sieve (0.074 mm). The grain size distribution in Figure 3.1 was obtained using ASTM D422-63 (ASTM, 1996a). Elemental analyses using X-ray fluorescence (XRF) are reported in Table 3.1.

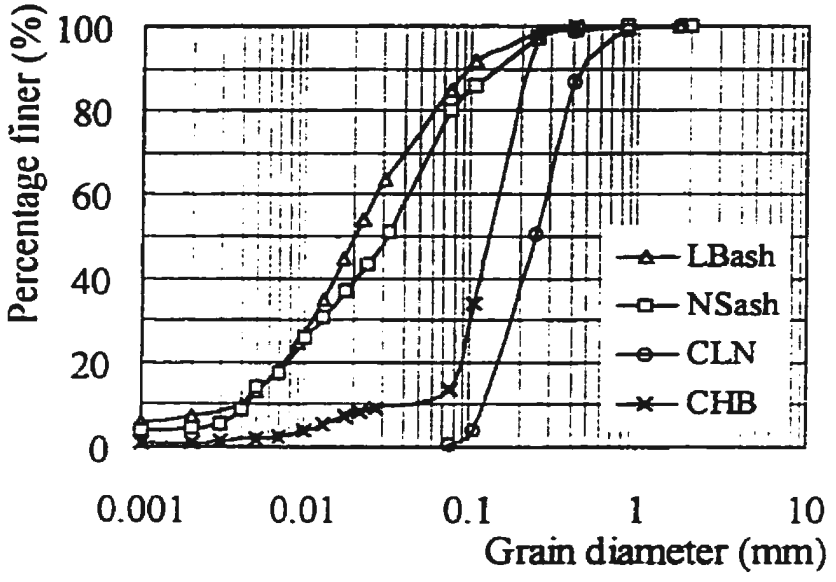

Figure 3.1 Grain size distribution

In these two fly ashes, Si, Al, and Fe are major elements. If calculated as oxides of the total mass, SiO_2 + Al_2O_3 + Fe_2O_3 accounts for 81.5% for LBash, and 84.8% for NSash. Their lime (CaO) contents are 4.7% and 1.6% respectively, which classify the two ashes into type F. The marked difference in elemental composition between the two ashes is that LBash is a high-carbon fly ash (Loss on Ignition, which is an indicator of unburnt carbon content, LOI=11.3%) but NSash is a low-carbon matter (LOI=2.2%). Unburnt carbon is an unwanted feature if ash is utilized in concrete, but the carbon becomes a welcome agent when the ash is used in contaminant containment.

Table 3.1 Elemental analysis converted to oxides (%) of the total mass

	LBash	NSash	Chabazite	Clinoptilolite
SiO_2	43.10	42.80	57.78	76.38
Al_2O_3	22.66	22.05	13.45	13.81
Fe_2O_3	15.71	19.96	9.94	1.62
CaO	4.67	1.61	1.32	3.64
Na_2O	1.05	0.68	6.62	0.25
MgO	1.30	1.57	2.10	2.34
K_2O	1.39	2.80	1.17	2.21
P_2O_5	0.27	0.12	0.02	0.04
TiO_2	1.29	0.99	0.20	0.26
MnO	0.03	0.07	0.10	0.05
LOI	11.30	2.20		

Fly ash mineralogy was determined by means of X-ray diffractometry (XRD). Aqueous suspension of LBash or NSash was air dried on a glass slide before X-ray scanning. The mass of ash solid on the slide was adjusted so that the relative intensity in the XRD pattern can be trusted. The XRD measurement was run in 3° ~ 70° 2θ scanning range at 1° 2θ/min (McCarthy, 1988). The XRD patterns are shown in Figure 3.2. In addition to a substantial amount of glassy matter, both ashes contain four major crystalline phases, i.e. quartz, mullite, hematite, and magnetite. These minerals are common species contained in typical Canadian coal fly ashes (Berry, 1978). It can be seen that the two XRD patterns in Figure 3.2 are almost identical except for the strong reflection at 2θ = 11.5° for NSash, which was identified as gypsum.

Scanning electron microscopy (SEM) is another desirable test in mineral characterization. SEM magnifies fine-grained ash particles by one thousand times, making the topographical observation objective and informative. The microstructure of LBash assemblage, as shown in Figure 3.3 (a), consists of glassy spheres and honeycomb-like textures. Most of the glass spheres are less than 15 μm in size. Deposition on the sphere surface contains mineral crystals. Individual mineral phases occur in small amounts, usually only a few percent of each type (Roy et al, 1985). The over-sized honeycomb structure is attributed to unburnt carbon fragments, which are irregular in shape and vesicular in appearance. Unburnt carbon constitutes a major part of the coarsest fraction of the ash particles. The voids contained in carbonaceous fragments may enclose fine fly ash spheres and mineral crystals. Because of high carbon content, LBash possesses a significant surface area, and therefore a large number of sorption sites.

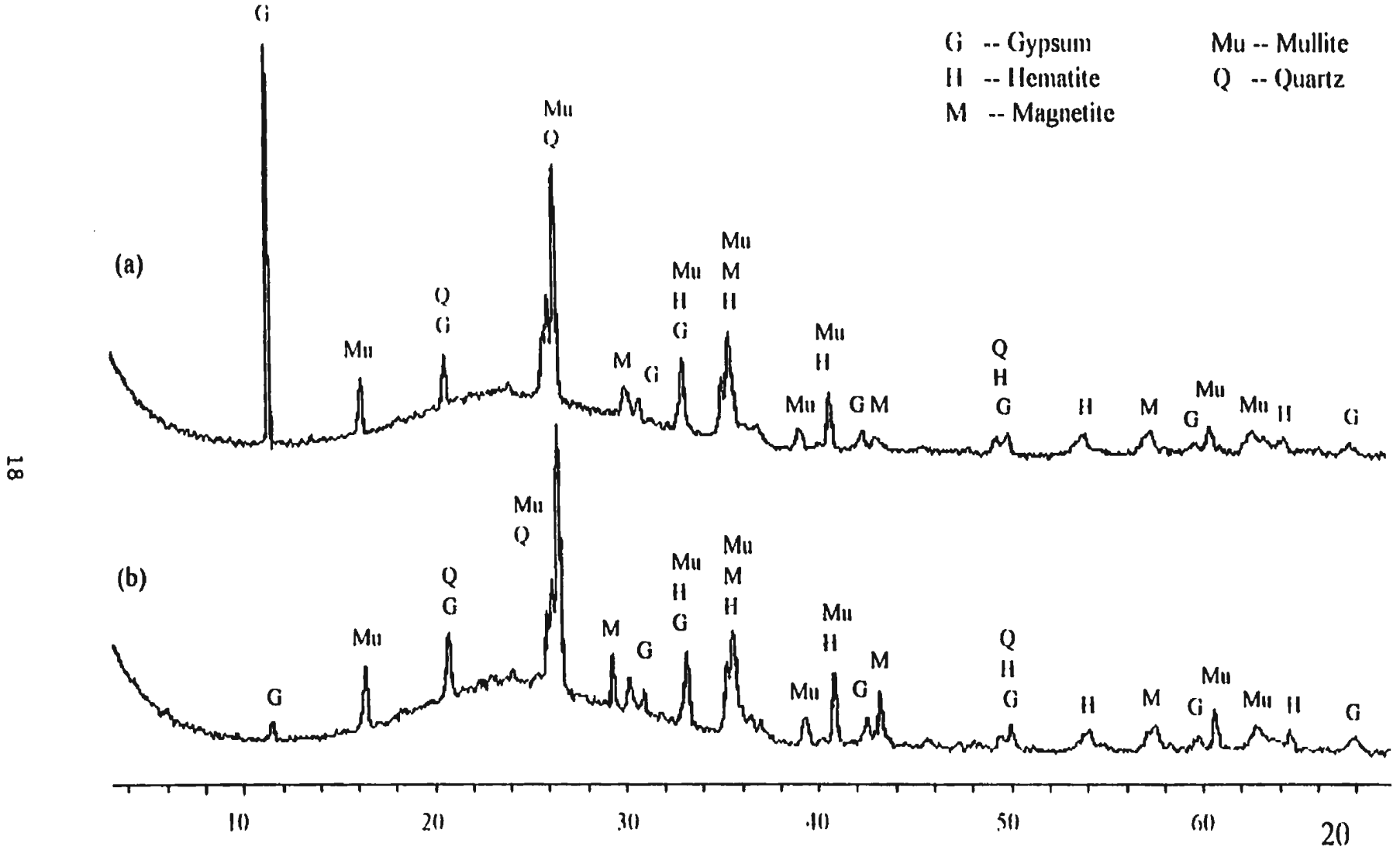

Figure 3 2 XRD patterns for (a) NSash and (b) LBash

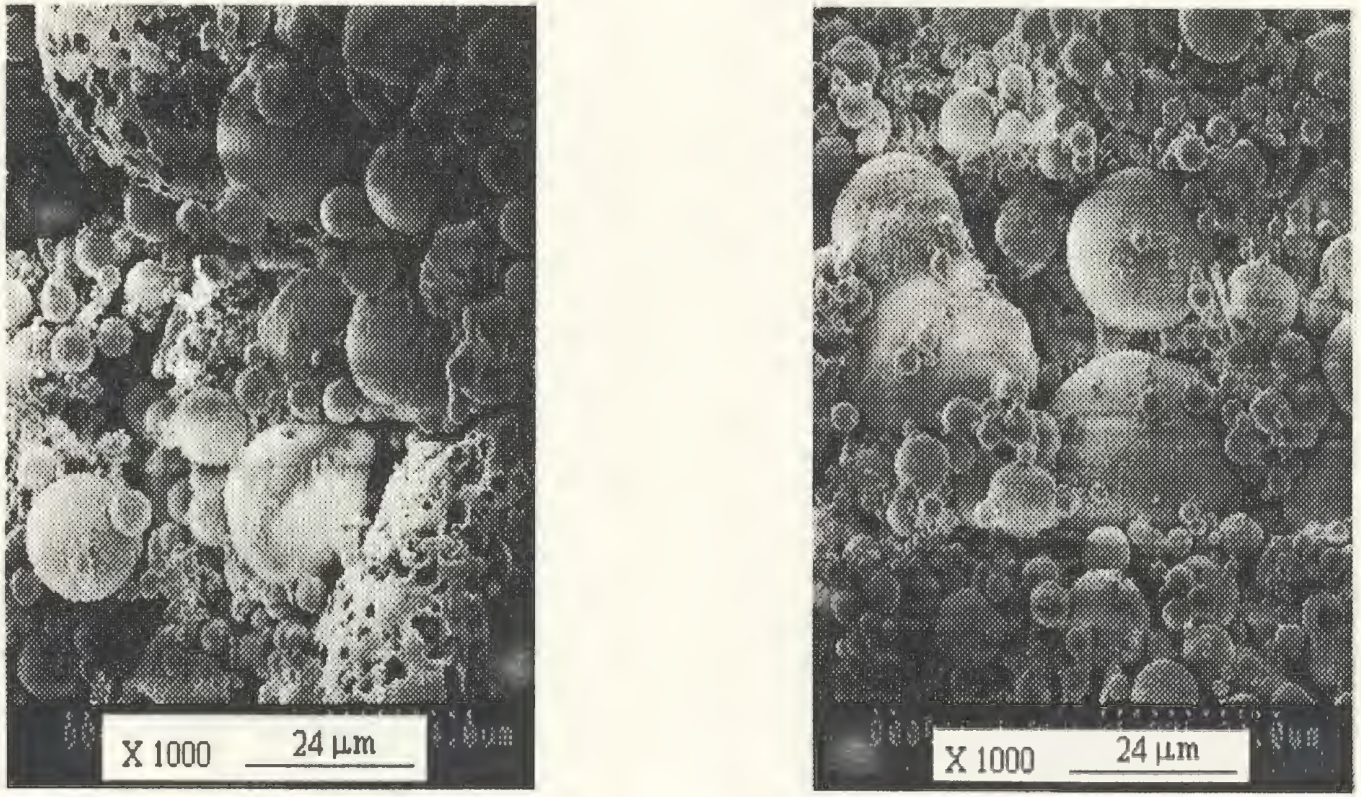

(a) LBash

(b) NSash

Figure 3.3 Microstructure of (a) LBash and (b) NSash

In comparison, the microstructure of NSash, as shown in Figure 3.3(b), consists merely of glassy spheres with deposition of crystal minerals. Spherical particles have a large range of size from less than 2 μm to 25 μm. No honeycomb-like structure is observed. Because of lower carbon content, NSash possesses a smaller surface area and has fewer sorption sites.

To make more detailed characterization, infrared (IR) spectra were measured for LBash and NSash. When infrared radiation excites molecules in an ash sample, bond vibrations take place in the molecules in the mode of bending or stretching, giving rise to an IR spectrum for structure determination. As a supplement to XRD and other instrumental methods, IR provides information about the identity of compounds that may be amorphous to X-rays. In particular, IR has the advantage in identifying functional groups on solid surface. Figure 3.4 is the IR spectra for LBash and NSash recorded with wave number (cm^{-1}) versus transmittance (%).

The three "peaks" (illustrated downward for each spectrum) at 2900, 1450, and 1375 cm^{-1}, respectively, correspond to the C-H absorption frequencies of "nujol" that was mixed with fly ashes during sample preparation. For LBash and NSash, absorption peaks in the range 1100 to 1000 cm^{-1} represent the main Si-O stretching in Si-tetrahedra; the broad peaks around 3300 to 3600 cm^{-1} are ascribed to the stretching vibration in O-H groups. LBash spectrum exhibits a peak near 1680 cm^{-1}, suggesting vibrations characteristic of the carboxyl group (-COOH, an organophilic functional group attached to unburnt carbon), but NSash spectrum shows this peak with negligible intensity.

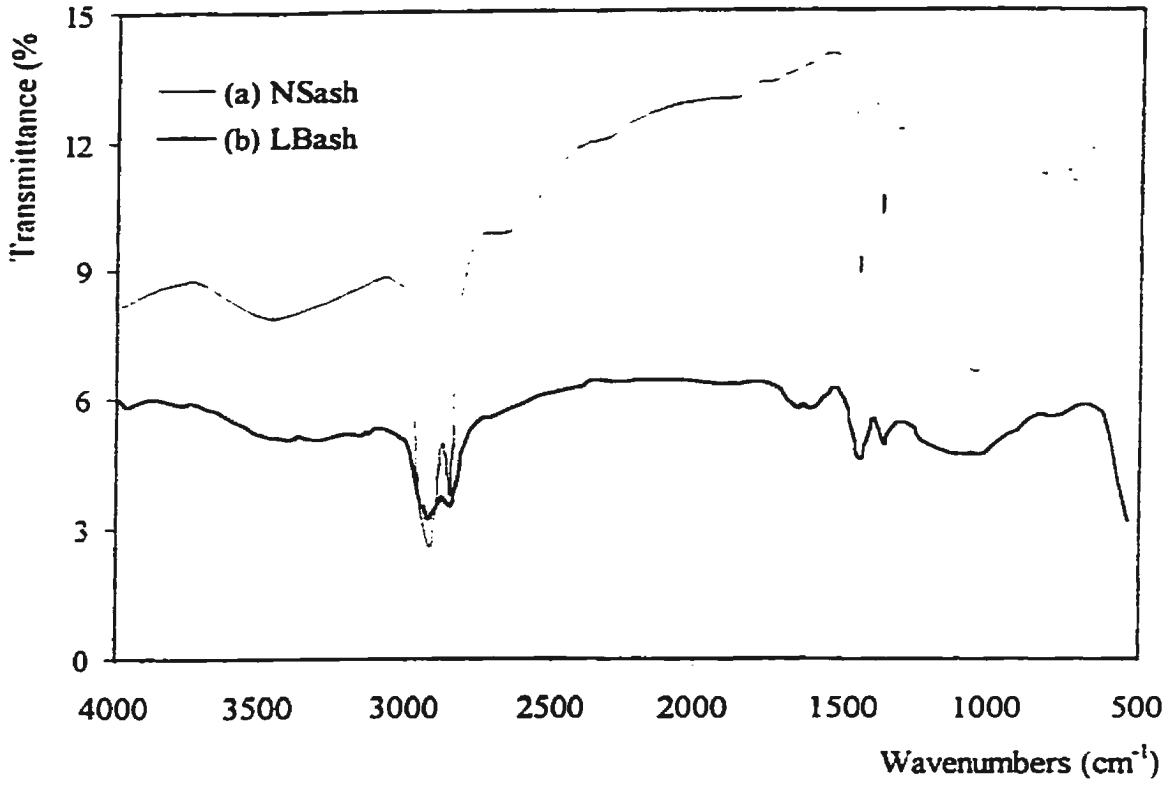

Figure 3.4 Infrared spectra for (a) NSash and (b) LBash

3.2 Zeolites

Two candidate zeolites, i.e. natural clinoptilolite and natural chabazite, were comparatively studied. Both materials were supplied by GSA Resources, Arizona. They were manufactured by crushing zeolite ores and screening the product through #20 sieve. Let CLN denote the natural clinoptilolite, and CHB the natural chabazite. As indicated in Figure 3.1, both zeolites are coarser in grain size than the aforementioned fly ashes. More than 86% of CHB and more than 99% of CLN are retained on #200 sieve.

Compositionally, zeolites can be distinguished according to their Si/Al (structural

cations) ratios and their K, Na, and Ca (exchangeable cations) contents. In aqueous solution, the activity or stability of zeolites is strongly associated with the Si/Al ratio of the structure. The high-silica or "acidic" zeolites are much more thermally stable and acid-resistant than low-silica or "basic" counterparts (Harkins, 1984). The exchangeable cation composition directly affects the cation exchange behaviour with given foreign cation species. Pure clinoptilolite, i.e. $KNa_2Ca_2(Si_{29}Al_7)O_{72}\cdot 32H_2O$, is a silica-rich zeolite that has a Si/Al ratio of 4.1. Its exchangeable cations are K^+, Na^+, and Ca^{2+}. Pure chabazite, i.e. $Ca_2Al_4Si_8O_{24}\cdot 12H_20$, is a silica-poor zeolite that has a smaller Si/Al ratio of 2.0. Its exchangeable cation is predominantly Ca^{2+}. However, the Si/Al ratio computed from Table 3.1 is 4.7 for CLN and 3.6 for CHB, neither agreeing with the formula Si/Al ratios. This is because CLN and CHB contain other intergrown silicate minerals as mined from natural deposits. Nevertheless, the trend of structural cation concentration reflected by XRF-deduced Si/Al ratios is the same as that reflected by the formula Si/Al ratios between the two zeolites. It is also likely that CLN and CHB contain "guest" ions of Na^+, K^+, Ca^{2+}, and Mg^{2+} in the exchangeable positions in their structures. Host and guest ions combine to form their working cation exchange capacity. Clinoptilolite has a lower cation exchange capacity (CEC) value corresponding to its large Si/Al ratio. For example, the CEC for CLN is 165 meq/100g, while the CEC for CHB is 250 meq/100g (Table 3.2), both being measured by the ammonium acetate method (Carter, 1993). The compositional information is summarized in Table 3.2.

Table 3.2 Compositional information for CLN and CHB

	Principal mineral	Exchan-geable cations	Si/Al		CEC (meq/ 100g)	Remark
			Formula based	XRF based		
CLN	Clinoptilolite	K^+, Na^+, Ca^{2+}	4.1	4.7	165	Not pure; high-silica; less active.
CHB	Chabazite	Ca^{2+}	2.0	3.6	250	not pure; low-silica; more active.

To ascertain the zeolite minerals and unknown impurities, XRD patterns were established for CLN and CHB using appropriate sample preparation methods. Because clinoptilolite often occurs along with heulandite, and both species belong to the same zeolite group with similar mineralogical structure, "heat treatment" needs to be applied to distinguish clinoptilolite from heulandite (Mumpton, 1960). During sample preparation, aqueous suspension of CLN was air-dried on two glass slides. One slide was directly scanned; another was heat treated at 550°C for 15 hours before scanning. Scanning of the two samples were run in 3~40° 2θ range at the speed of 1° 2θ/min (Bole, 1972). From the XRD pattern of the air-dried sample, clinoptilolite, Ca-heulandite and [Ca, Sr]-heulandite, barrerite, and stellerite were qualitatively identified, as illustrated in Figure 3.5(b). From the XRD pattern of the heat treated sample, clinoptilolite was still recognized, but no heulandite reflection remained identifiable due to the complete destruction of the heulandite structure under prolonged high temperature, as shown in

Figure 3.5 (c). The comparison of the two scanning results proved the paragenesis of clinoptilolite and heulandite in the original CLN sample.

Air-drying aqueous suspension on a glass slide is an acceptable way to prepare a chabazite sample. From the XRD pattern of CHB in Figure 3.5(a), chabazite was identified as a major zeolite phase; another three zeolites were revealed as minor phases, i.e. clinoptilolite, heulandite, and probertite.

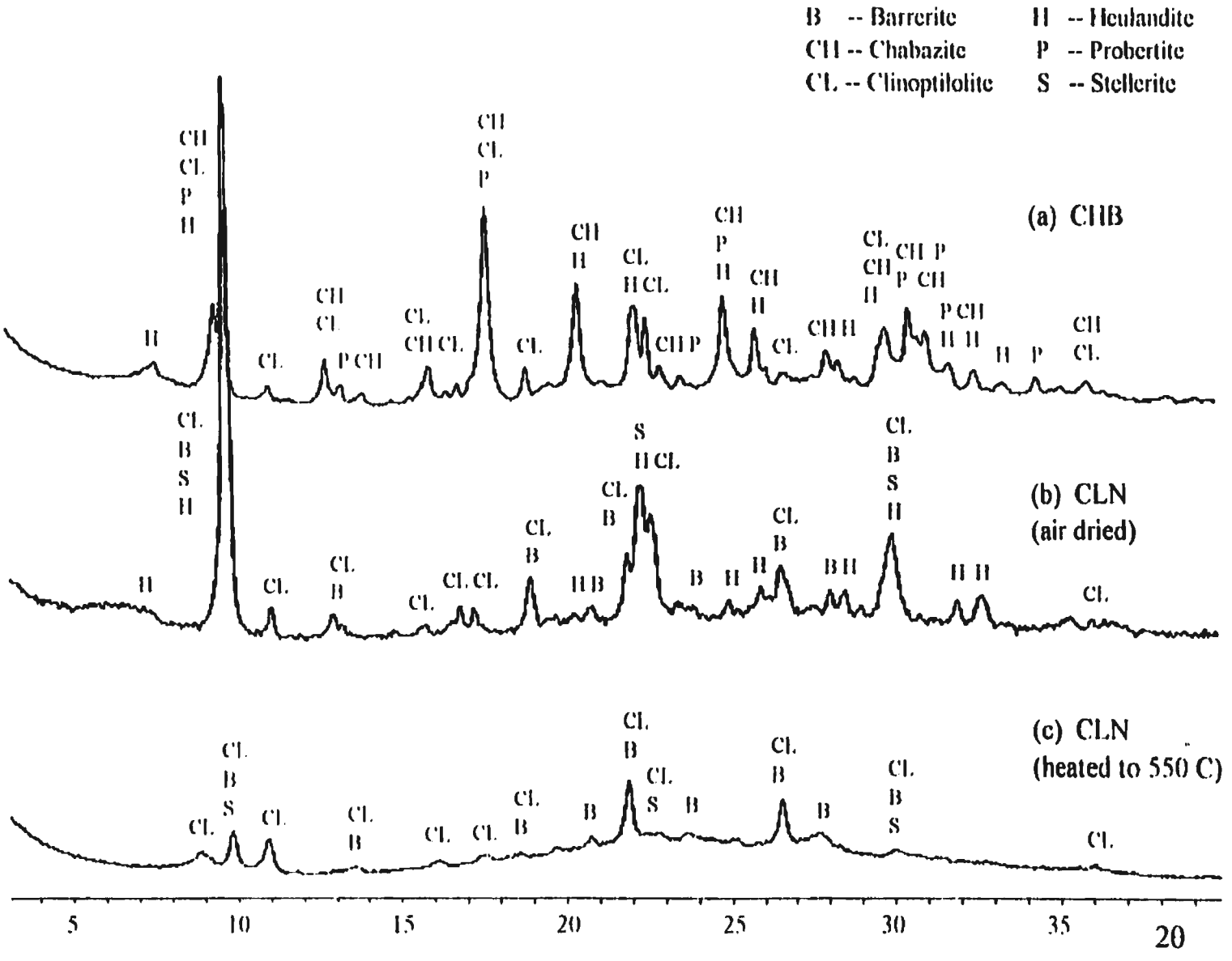

Figure 3.5 XRD patterns for (a) CHB and (b) (c) CLN

SEM is an ideal device to observe the size and texture of fine-grained zeolite assemblages. It is also useful to qualitatively address the abundance of the zeolite concerned. The morphology of CLN and CHB is shown in Figure 3.6. Typical clinoptilolite crystals display characteristic monoclinic symmetry, and they are mostly coffin-like in shape, as shown in the upper part of Figure 3.6(a) zoomed from the lower part of the same figure. In CLN, however, clinoptilolite crystal was found not very abundant over the entire area of the sample scanned. Fragments of non-zeolitic impurities could be observed. This means that CLN is not a high grade clinoptilolite. When the CHB sample was examined with SEM, a large number of cube-like rhombohedra was detected, as shown in Figure 3.6(b). Typical chabazite is characterized by such "cube" or "rhomb" crystals with an average size of 5 μm. The cube-like shape was fostered in sediments from saline-lake or marine environment. Impurities intergrown with prevailing chabazite crystals are unreacted volcanic glass (ash). Anyhow, CHB can still be considered of high grade in chabazite. The SEM-based assessment on zeolite abundance is consistent with the compositional analysis in Table 3.2.

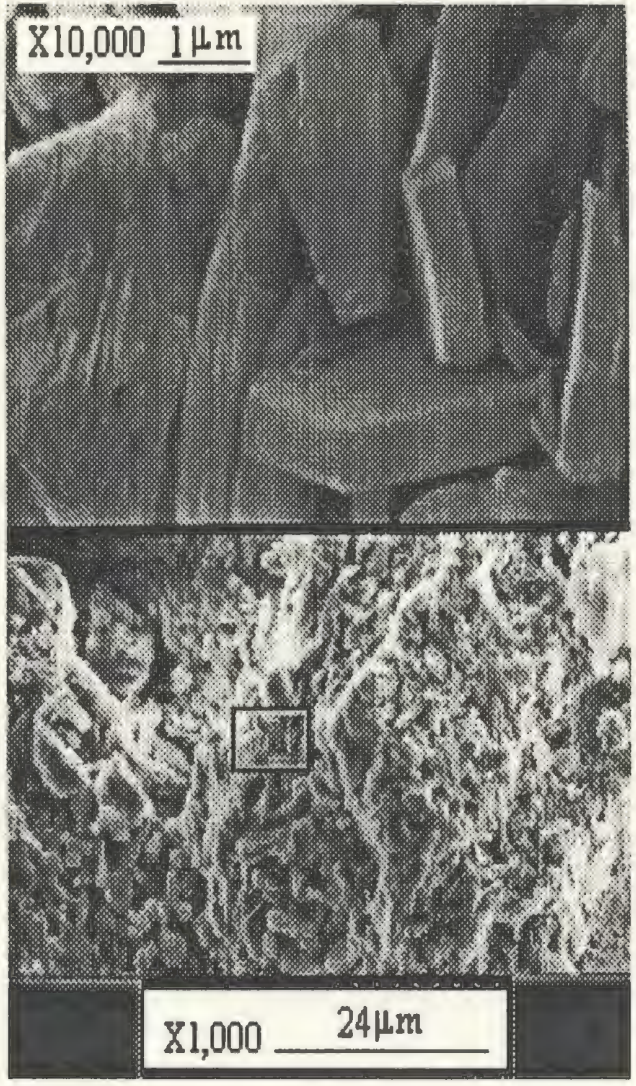

(a) CLN

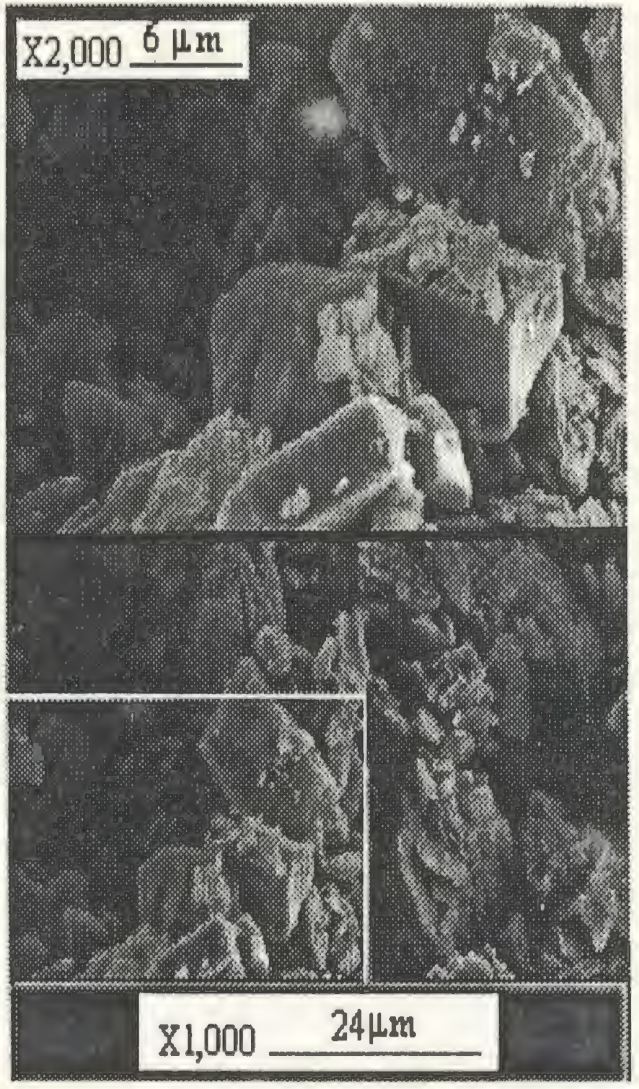

(b) CHB

Figure 3.6 Microstructure of (a) CLN (clinoptilolite) (b) CHB (chabazite)

The IR measurements for CLN and CHB are presented in Figure 3.7. Peaks at 720 cm^{-1} and 800 cm^{-1} may be due to CO_3^{2-} vibration; peaks in the range 1100 to 1000 cm^{-1} are attributed to Si-O stretching in Si-tetrahedra; another significant peak exists at 1650 cm^{-1} for CHB or at 1640 cm^{-1} for CLN, indicating that H-O-H bending requires lower energy in the latter. Between the band 3700 and 3200 cm^{-1} are absorption peaks due to O-H stretching that requires higher energy. The identification of H-O-H and O-H groups confirms the hydration water and hydroxyl functional groups in zeolite minerals.

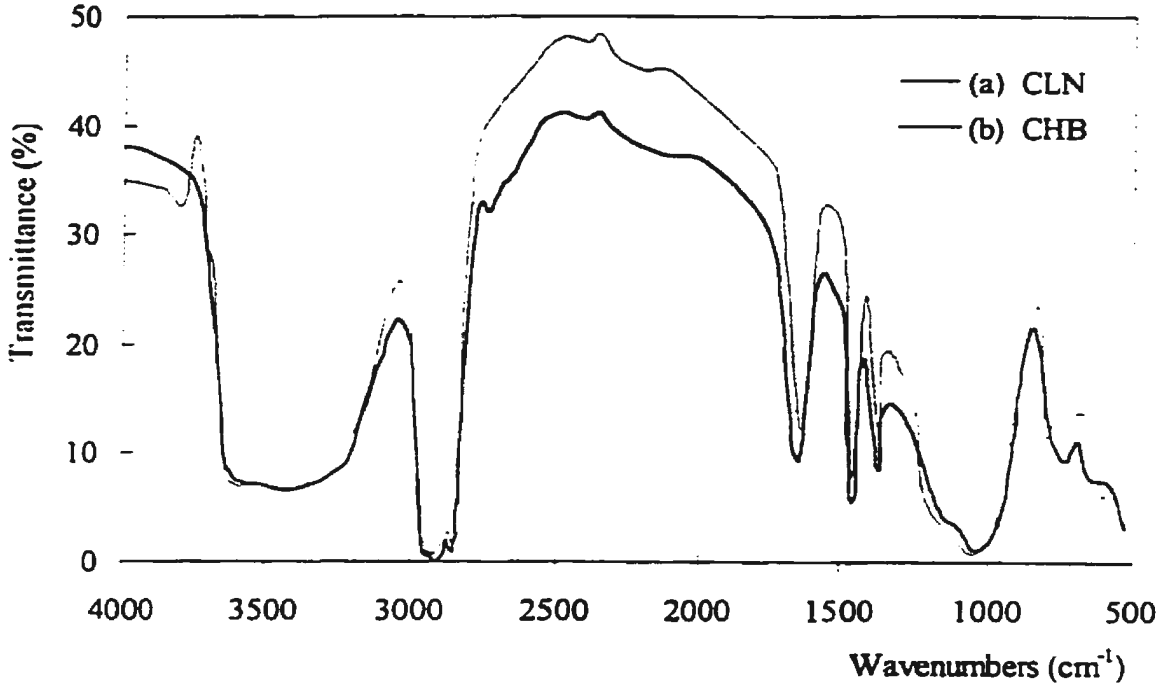

Figure 3.7 Infrared spectra for (a) CLN and (b) CHB

3.3 Summary of Materials

To summarize the characterization of the four candidate materials, LBash has higher carbon content, larger surface area, and more organophilic functional groups, than NSash; CHB shows better grade of zeolite purity, higher chemical activity, and larger CEC value, than CLN. Therefore, during the subsequent experimental stage, in-depth studies were focused on LBash, CHB, and their mixes, although NSash and CLN were sometimes involved for comparative purpose.

3.4 Synthetic Leachates

The chemical properties of MSW leachates are highly complex and variable. In LaGrega's (1994) summarizing report, as many as 10 inorganic substances and 25 organic compounds were listed that could be detected in landfill sites with wide range of concentrations. For example, Pb^{2-} might range from 0 to 19 mg/l; phenol from 0 to 17 mg/l. Tests of liners using real leachate would not allow easy interpretation of the results. Therefore, the synthetic leachates in this study were prepared in three distinct forms: Pb^{2-} solution as leachate-1, phenol solution as leachate-2, and mixture of Pb^{2-} and phenol as leachate-3.

Lead and phenol were chosen to represent to a certain extent the inorganic and organic constituents of leachate contaminants. Lead is one of the most extensively used heavy metals, for example, in plumbing and lead-acid batteries. Once released into the environment, lead is not subject to chemical and biological destruction, but becomes a persistent contaminant. Consequences of lead poisoning include damage to the kidney

and central nervous system, to which children are most susceptible.

Phenol (C_6H_5OH) molecule has a polar property, making it very soluble in water and mobile in the environment. With ionization constant (pKa) of 10, phenol is a stronger acid than alcohol but weaker than carboxylic acids. Being an important industrial chemical itself and the parent of a large class of phenolic compounds, phenol is used in plastics, paints, dyeing, pharmacy, and pesticides. Not surprisingly, it becomes one of the most commonly encountered organic pollutants. Phenol is toxic by ingestion, inhalation, and skin absorption, and is a strong irritant to dermal tissues. It gives unpleasant taste and odour to drinking water even at the parts per billion level (Singh et al, 1994).

In order to test the long term behaviour of zeolite and fly ash in the presence of concentrated leachates, the three synthetic leachates were prepared at elevated concentrations, i.e. Pb^{2+} = 2500 mg/l using $Pb(NO_3)_2$ for leachate-1 and leachate-3, and phenol = 55 mg/l for leachate-2 and leachate-3. In the following text, *ppm* will be employed in place of *mg/l*. The pH of leachate-1 (Pb^{2+} at 2500 ppm) is 5.3; the pH of leachate-2 (phenol at 55 ppm) is 6.5. In leachate-3 (Pb^{2+} at 2500 ppm and phenol at 55 ppm), Pb^{2+} and phenol interact to form Pb-phenol complex. The complexation releases an appreciable amount of H^+ from the hydroxyls of phenol molecules. The H^+ concentration in leachate-3 is thus increased and its pH decreases to 4.5.

4 EXPERIMENTAL PROCEDURES

The sorption and hydraulic conductivity of zeolite and fly ash with concentrated synthetic leachates were investigated experimentally through batch equilibrium test, column leaching test, hydraulic conductivity measurement, and differential extraction of sorbed Pb^{2+}.

4.1 Batch Tests with Pb^{2+}

Batch tests were conducted on LBash, NSash, CHB, and CLN, respectively, to estimate the extent of Pb^{2+} sorption from solutions by each of the four sorbents at equilibrium. Lead solution series had concentrations of 1,000, 2,000, 3,000, 4,250, 6,000, 12,000, 16,000, 20,000, 35,000, 50,000 ppm for the tests on LBash and CHB, and 600, 1,000, 1,500, 2,000, 2,500, 3,000, 3,500, 4,250, 6,000 ppm for NSash and CLN.

Eleven grams of air-dried solid was placed into each of a series of 125 ml conical flasks. Then 110 ml of one of the serial Pb^{2+} solutions was transferred into each flask. The solid:solution ratio became 1:10 in accordance with the USEPA recommendations (Roy et al, 1991). The solid and solution filled about 80% to 90% of each flask, therefore the container surface involved in the sorption reaction was limited. Flasks with no sorbent but containing 110 ml Pb^{2+} solution of a corresponding concentration were employed as blanks to control the accuracy of sorption estimation. After 24 hours agitation facilitated by means of a reciprocal shaker (Roy et al, 1991), adequate contact was achieved between Pb^{2+} ions and zeolite (or fly ash) solids, and sorption and desorption reached equilibrium at solid-liquid interfaces. The test proceeded with

centrifugation at 2200 r.p.m. to separate the equilibrium Pb^{2+} solutions from suspensions. The supernatants were preserved in polypropylene bottles at pH<2 adjusted by HNO_3. Finally, an atomic absorption spectrophotometer (AAS) was used to quantify the Pb^{2+} concentrations in the equilibrium solutions. Initial Pb^{2+} concentrations were corrected by the final blank concentrations to eliminate the error caused by sorption onto the glassware surface. Differences between the corrected initial Pb^{2+} concentrations and corresponding equilibrium concentrations provided the basis for the construction of sorption isotherms. The amount of Pb^{2+} sorbed per mass of zeolites (or fly ashes), or C^*, was determined by

$$C^* = \frac{C_e - C_b}{m} V_f \qquad (4.1)$$

where C_e is the Pb^{2+} concentration after exposure to a sorbent upon equilibrium; C_b is the Pb^{2+} concentration after the blank is agitated for 24 hours; m is the mass of the sorbent in a flask converted to oven-dried basis; and V_f is the volume of Pb^{2+} solution in the flask.

4.2 Batch Tests with Phenol

Physicochemical stability of phenol in solution should be taken into account in the related batch sorption procedures. The stability problem mainly arises from processes such as photolysis and/or microbial degradation. Microbial degradation is closely associated with the nature of sorbents involved. For example, biodegradation of phenol increases linearly or exponentially with time when sorbents are nonsterile soils, but phenol biodegradation is negligible when sorbents are sterile soils (Scott et al, 1982). Overall,

degradations resulting from different mechanisms lead to a decrease in phenol concentration concomitantly with sorption. Precaution should be taken to control phenol instability relative to the batch technique.

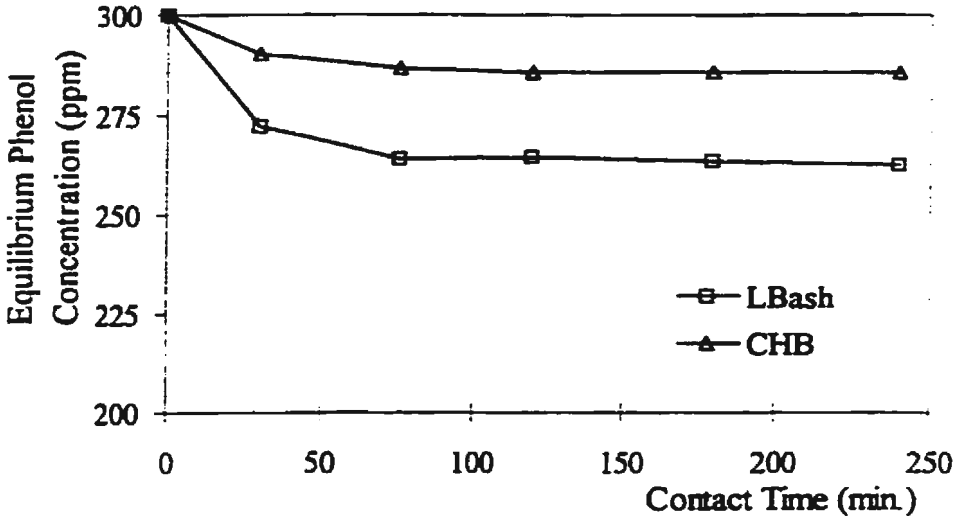

Figure 4.1 Contact time versus phenol sorption

In the current phenol sorption batch tests, the solid-to-solution ratio was also set at 1:10. Appropriate measures were adopted to maintain the physicochemical stability of phenol with fly ashes and zeolites as sorbents. Reaction containers (flasks) were wrapped with aluminum foil to avoid laboratory light. The equilibration time of 1.5 hours was chosen from literature recommendation (Singh et al, 1994), and verified by an iterative process (Figure 4.1). Agitation of 1.5 hours not only established equilibrium phenol concentration in the solid-liquid suspension, but also limited the potential influence of

degradation. Blanks holding no sorbent but specific phenol solutions were tested under identical conditions to account for probable degradation losses. The equilibrium phenol concentrations in supernatants (C_e), and final blank concentrations (C_b) were measured with ultraviolet spectrophotometry at the wavelength of maximum absorption, namely 270 nm. The amount of phenol sorbed per mass of zeolites (or fly ashes) can also be calculated by equation (4.1).

4.3 Leaching Tests

Unlike batch equilibrium test in which adequate agitation is facilitated and all the sorption sites of a sorbent are involved to yield an ideal sorption isotherm, a leaching test simulates the sorption phenomenon by sorbate permeation through a sorbent column that permits contaminant migration and sorption simultaneously. Since the sorbent is no longer loose in the packed column, not every single solid particle or sorption site is exposed to sorbate when the sorbate solution is infiltrating through sorbent pores and voids. The equilibrium sorption so established may not result in as much retention of sorbate as observed in a batch test, but the configuration of the leaching test is more analogous with the real liner situation.

4.3.1 Permeameter

Fixed-wall permeameters were used in this research because of their applicability as leaching cells and relatively low cost. A schematic diagram of the device along with inflow/outflow units and pressure supply is shown in Figure 4.2.

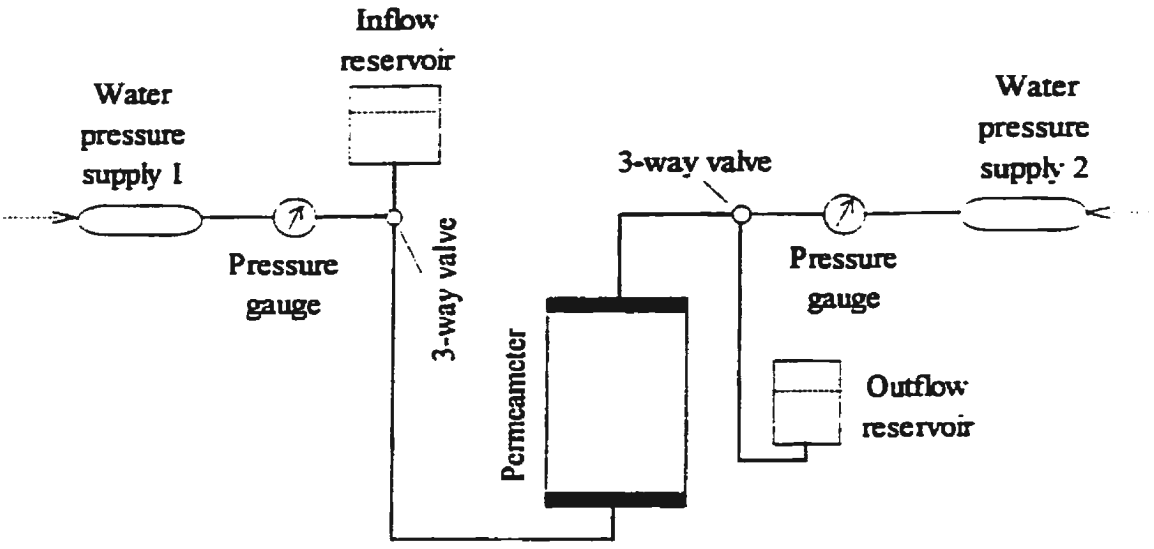

Figure 4.2 Fixed-wall permeameter setup

Each permeameter was made of a cast acrylic ring 2.54 cm (1.0 in.) long and 5.08 cm (2.0 in.) in diameter, and top and bottom acrylic plates clamped together with eight nuts screwed onto four aluminum all-thread rods. The ring can be easily assembled with a new sorbent specimen or dismantled with a sorbate-saturated specimen. Two porous disks were attached to the two end plates respectively, facing the specimen in the ring. The lucite ring permitted observation of the specimen during leaching. In addition, the seal between the ring and end plates was provided by Viton O-rings that are chemically resistant. Polyethylene tubings were used for inflow and outflow. The Pb^{2+} permeant of 2500 ppm is chemically compatible with all parts of the permeameter. Phenol solution could be severely corrosive to acrylic ring for concentrations higher than 10,000 ppm, but

phenol in 55-ppm aqueous solution like leachate-2 and leachate-3 did not cause chemical attack to acrylic or any other part of the permeameter system.

To remove the entrapped air and saturate the specimen with water, an extended period of back-pressure was applied to the permeameter prior to the start of a leaching test.

4.3.2 Specimen Preparation

Compaction behaviour of zeolites and fly ashes had to be understood before preparing leaching test specimens into permeameters. LBash, NSash, CHB, and CLN were compacted, respectively, following ASTM standard procedures (ASTM D698-91, ASTM, 1996b). As indicated in Figure 4.3, more than 9 incremental water contents were used to construct a complete compaction curve for each material, so that the maximum dry densities and the optimum water contents can be determined with certainty. Although LBash has a larger specific gravity than NSash (see Table 4.1), the compacted dry density for LBash is lower than that for NSash. This in turn proves the influence of hollow particles in LBash. Accordingly, LBash has a larger optimum water content than NSash. Compared with CLN, CHB has a lower maximum dry density and larger optimum water content due to its lower Si-content, lower specific density, and more micro-pores. Some index properties of zeolites, fly ashes, and their mixtures are summarized in Table 4.1, including specific gravity, maximum dry density, optimum water content, and void ratio at standard compaction.

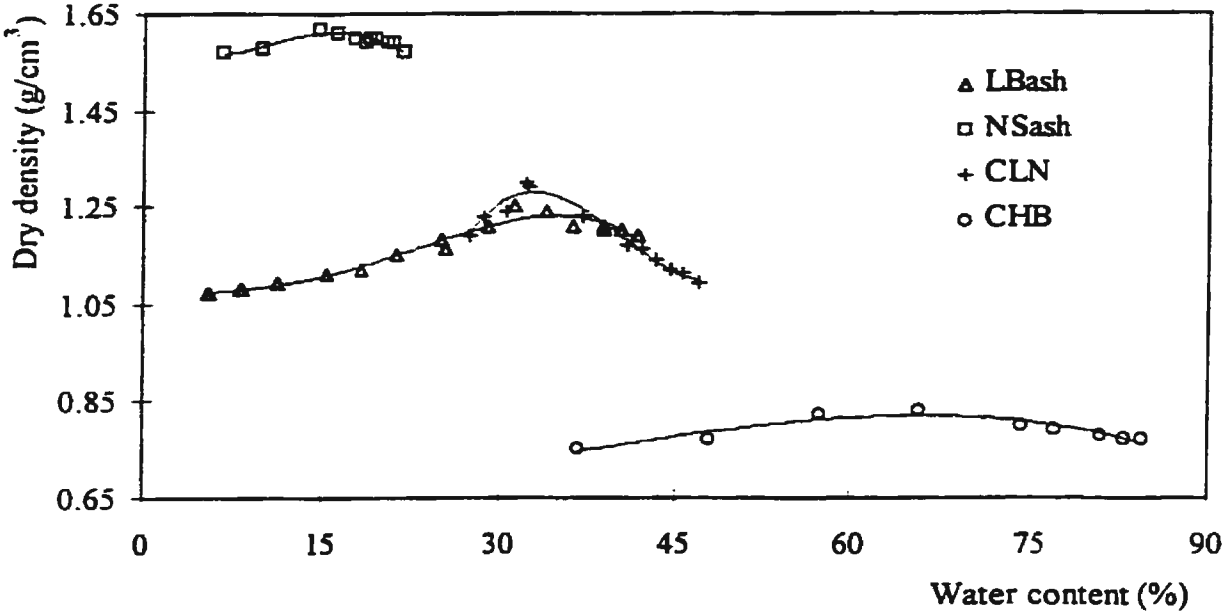

Figure 4.3 Standard compaction curves

Table 4.1 Some index properties of zeolites, fly ashes, and their mixtures

	Specific gravity (g/cm^3)	Maximum dry density (g/cm^3)	Optimum water content (%)	Void ratio as compacted
LBash	2.55	1.24	34	1.06
NSash	2.35	1.62	15	0.45
CLN	2.46	1.28	33	0.92
CHB	2.32	0.83	65	1.80
30%LBash+70%CHB	2.39	-	-	1.75
50%LBash+50%CHB	2.44	-	-	1.60
70%LBash+30%CHB	2.48	-	-	1.41

In light of material compaction properties, individual specimens were prepared with LBash, NSash, CLN, CHB, and each of the three LBash-CHB mixes mentioned in Table 4.1, respectively. Each test material was directly compacted into a permeameter ring to minimize the side-wall leakage. Totally, thirteen specimens were prepared, each being done only when vacant permeameters were available. All specimens were at water contents close to optimums and had dry densities of 95%-103% of the corresponding maximum dry densities. Some individual dry densities slightly exceeded the "maximum" values indicated in their corresponding compaction curves, due to a compaction effort applied to the specimen which was greater than the effort used in standard compaction. For the sake of identification, specimens were named according to the material used, the weight percentage of each material in a mixture, and the leachate to be leached to the specific specimen. LB and NS were used to denote LBash and NSash respectively. CLN and CHB, previously used to represent two zeolites, were also assigned for specimen identification. CHB-1, for example, refers to a specimen of pure CHB to be permeated with leachate-1; LB3:CHB7-2 refers to a mixture specimen of 30% LBash and 70% CHB with leachate-2. Information on the thirteen specimens as prepared is listed in Table 4.2.

Table 4.2 Details of thirteen specimens as prepared

Specimen I.D.	Material	Leachate*	Dry density as compacted (g/cm^3)	Void ratio
LB-1	LBash	Leachate-1	1.20	1.13
NS-1	NSash		1.56	0.50
CLN-1	CLN		1.21	1.03
CHB-1	CHB		0.80	1.91
LB3:CHB7-1	30%LBash+70%CHB		0.88	1.71
LB5:CHB5-1	50%LBash+50%CHB		0.90	1.72
LB7:CHB3-1	70%LBash+30%CHB		1.03	1.41
LB-2	LBash	Leachate-2	1.19	1.13
CHB-2	CHB		0.77	2.00
LB3:CHB7-2	30%LBash+70%CHB		0.90	1.65
LB5:CHB5-2	50%LBash+50%CHB		0.92	1.64
LB7:CHB3-2	70%LBash+30%CHB		1.00	1.49
LB5:CHB5-3	50%LBash+50%CHB	Leachate-3	0.94	1.58

* In leachate-1, Pb^{2+} = 2500 ppm;

in leachate-2, phenol = 55 ppm;

in leachate-3, Pb^{2+} = 2500 ppm, and phenol = 55 ppm.

4.3.3 Hydraulic Conductivity Measurement and Effluent Sampling

Following the preparation of each specimen, it was saturated with distilled water. The saturation was facilitated by using a 200 kPa backpressure for 24 hours, during which slow permeation of water flushed the dissolved air out of specimen voids. Upon water saturation, the specimen was subjected to percolation of a specific leachate under an imposed hydraulic gradient. The gradient was increased from about 10 to an appropriate value to expedite the leaching process. The increase was made by using small increments to allow for pore pressure equilibration within the specimen. To avoid erroneous measurement of hydraulic conductivities, the hydraulic gradient was kept low enough to avoid migration of solid particles that could result in clogging of pore space or erosion of the test material. The effluent solution was collected and weighed at appropriate time intervals. The hydraulic conductivity, K (m/s), of the test specimen in the individual time period was then computed on the basis of Darcy's law, i.e.

$$K = \frac{V_i}{A \cdot \Delta t_i} \frac{L}{h_I} \qquad (4.2)$$

where L = length of the specimen (m); A = cross-sectional area of the specimen (m^2); Δt_i = individual time interval (s); h_i = average head difference between inflow and outflow during Δt_i; V_i = the effluent volume collected during Δt_i.

Meanwhile, the effluent solution was sampled for chemical analysis, which served to indicate the amount of Pb^{2+} or phenol sorbed by the specimen, and the interaction between sorbent minerals and the leachate constituents. The criteria to terminate a leaching test were as follows: the hydraulic conductivity must be stabilized in time; the

concentration of Pb^{2+} or phenol in the effluent solution must equal that in the influent solution.

4.3.4 Sequential Extraction for Pb-partitioning

After the termination of each leaching test in which the permeant was leachate-1 or leachate-3, the Pb^{2+} saturated specimen was dismantled from the permeameter. There remained a strong need to differentiate chemical partitions (or speciations) of total Pb^{2+} retained on fly ash and/or zeolite solids, such that the relative role of different sorption sites could be better appreciated, and the disparity of different sorbent materials in Pb^{2+} retention could be interpreted. This was accomplished by using a sequential extraction procedure (Yong et al, 1992). From the viewpoint of sequential extraction, heavy metals sorbed on mineral solids can be divided into several fractions, each being associated with specific sites with specific binding strength. Appropriate extraction agents can be used sequentially, each extractant destroying only bindings of specific strength but leaving other bindings unattacked. Thus, individual metal fractions can be detected one after another Recently, Gasser et al (1996) suggested to distinguish Pb-sorbent association into four fractions as follows:

Fraction 1 -- exchangeable: Pb^{2+} ions of this fraction are considered to be non-specifically sorbed and exchangeable. Neutral salts such as $MgCl_2$ and $CaCl_2$ are suitable ion-displacing extractants to release Pb^{2+} physically bound by electrostatic attraction to the negatively charged sites on solid surfaces. The cation concentration in the extractant solution should be high enough to displace the exchangeable Pb^{2+}.

Fraction 2 -- associated with amorphous silicates or organic matter: Pb^{2+} ions are attached to amorphous silicate phases, and moderately fixed via precipitation. The binding mechanisms for Pb^{2+} in association with organic matter include complexation, adsorption, and chelation. Sodium hydroxide can be an optional extractant for this fraction.

Fraction 3 -- associated with oxides: Pb^{2+} ions are retained to amorphous or poorly crystallized Fe, Al, and Mn oxides. These oxides exist as nodules, concretions, cement between particles, or coating on particles. They serve as excellent scavengers for trace metals. Pb^{2+} precipitation of this fraction is relatively strongly bound, but can be dissolved by EDTA extraction.

Fraction 4 -- internal: Pb^{2+} ions are held within the crystal structure of silicate minerals which consist mainly of primary/secondary minerals resistant to the extractions of fraction 1, 2, and 3. Pb^{2+} ions of this fraction are not expected to be released from preceding extractant solutions, but can become extractable after digestion with strong acids (i.e. HNO_3) at elevated temperatures. For average soils, heavy metal sorption associated with this fraction is usually not significant, but it is needed in mass balance assessment.

Gasser's sequential extraction scheme (Gasser et al, 1996) has been used in this study, as outlined in Table 4.3.

Table 4.3 Sequential extraction scheme

Pb fraction	Extractant	Procedure*
Fraction 1 -- exchangeable	$MgCl_2$	Add 30 ml of 1 M $MgCl_2$ to 0.5 g of sorbent solid; shake 2 h; centrifuge; quantify Pb by AAS
Fraction 2 -- associated with amorphous and organic matter	NaOH	After weighing the residue of $MgCl_2$ extract, add 30 ml of 0.5 M NaOH; shake 2 h; centrifuge; quantify Pb
Fraction 3 -- associated with oxides	EDTA	After weighing the residue of NaOH extract, add 30 ml of 0.05 M Na_2EDTA; shake 2 h; centrifuge; quantify Pb
Fraction 4 -- internal	HNO_3	After weighing the residue of EDTA extract, add 30 ml of 4 M HNO_3; shake gently for 24 h; heat 4 h at 80°C; centrifuge; quantify Pb
* The residual amount of extraction solution trapped after decanting a centrifuged extract was determined gravimetrically. The amount of Pb trapped in this residual solution was accounted for by calculation.		

5 RESULTS

In the following sections, the sorption isotherms of Pb^{2+}/phenol for fly ash and zeolites in batch tests will be presented; then the hydraulic conductivity measurements from column leaching tests will be introduced, followed by sorption data plus pH observations from Pb^{2+}/phenol leaching tests.

5.1 Pb^{2+} Sorption Isotherms

By using Eq. (4.1), sorption data from batch tests were expressed as sorption isotherms, which are graphical representation of the relationship between the sorbate concentration in the equilibrium solution and the amount of sorbate taken up by sorbent solids (i.e. fly ash or zeolite). As shown in Figure 5.1(a), NSash and CLN underwent a series of original Pb^{2+} solutions between 600 and 6000 ppm before NSash was saturated at about 28 mg-Pb per gram of ash solid, and CLN saturated at about 21 mg-Pb per gram CLN solid. CHB and LBash sorbed almost all the Pb^{2+} ions from original solutions between 1,000 and 4,250 ppm. They remained unsaturated until the original Pb^{2+} solution was as concentrated as 50,000 ppm (Figure 5.1(b)).

5.2 Phenol Sorption Isotherm

Figure 5.2 (a) to (d) show phenol sorption isotherms of LBash, NSash, CHB, and CLN. LBash was found to be the most effective material that had an equilibrium capacity of about 1.30 mg/g (i.e. mg-phenol per gram sorbent), followed by CHB (0.45 mg/g), CLN (0.27 mg/g), and NSash (0.20 mg/g). The four isotherms in Figure 5.2 appear as

"S" type. Namely, each of them rises slowly in the initial stage, then ascends more steeply, and finally levels off upon saturated sorption.

The two sets of sorption isotherms in Figure 5.1 and 5.2 represent the ideal sorption potentials of candidate materials. In view of their potential sorption capacities and the mineralogical characteristics described in Section 3, LBash and CHB were given preference as liner construction materials.

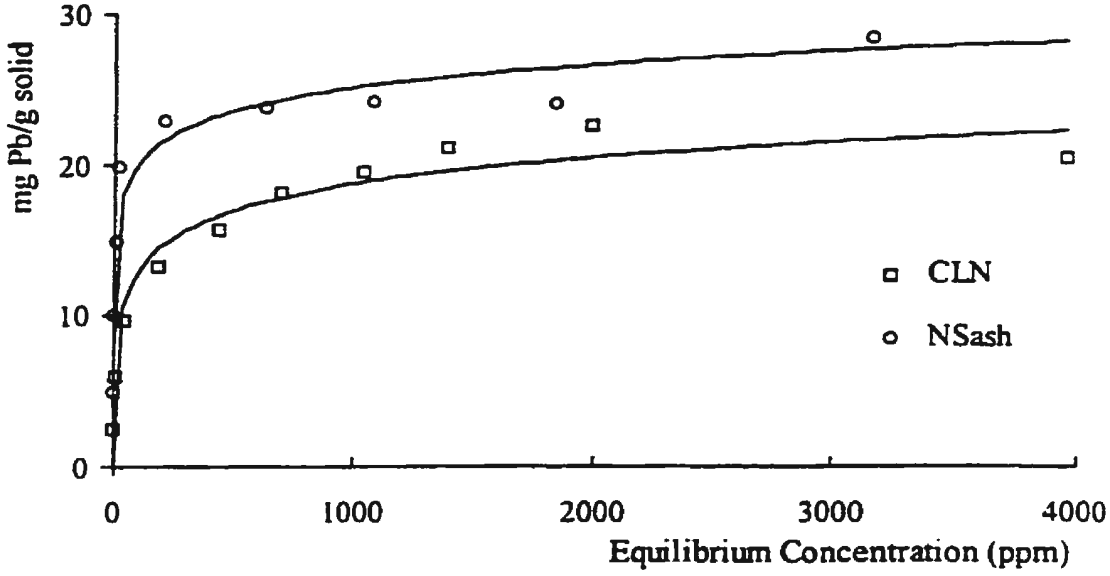

(a) CLN and NSash

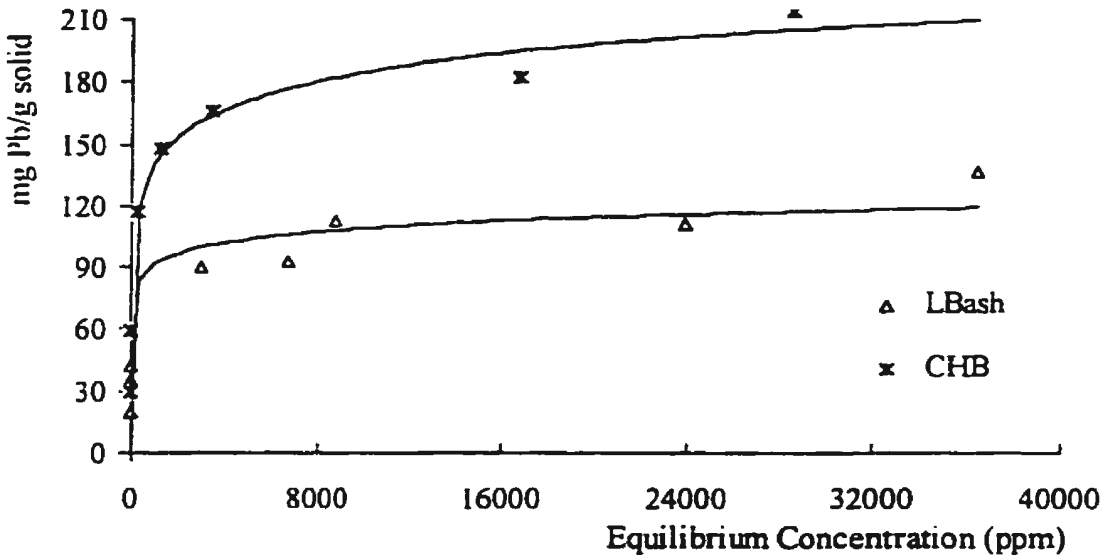

(b) CHB and LBash

Figure 5.1 Sorption isotherms from batch tests with Pb^{2+}

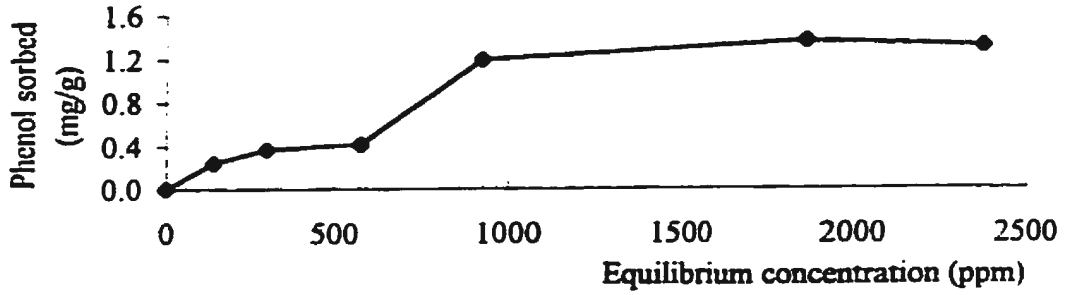

(a) Batch test for LBash with phenol

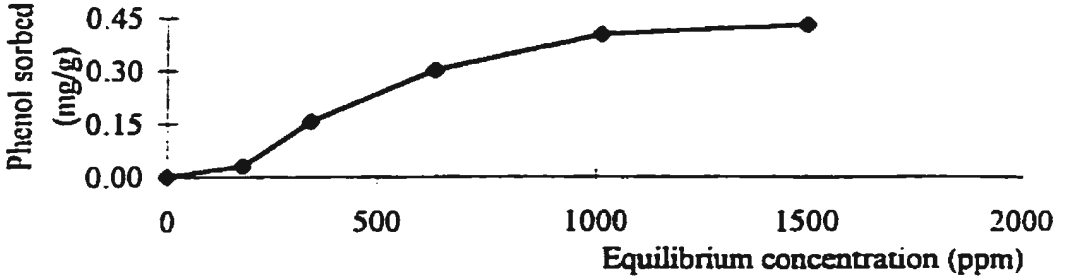

(b) Batch test for CHB with phenol

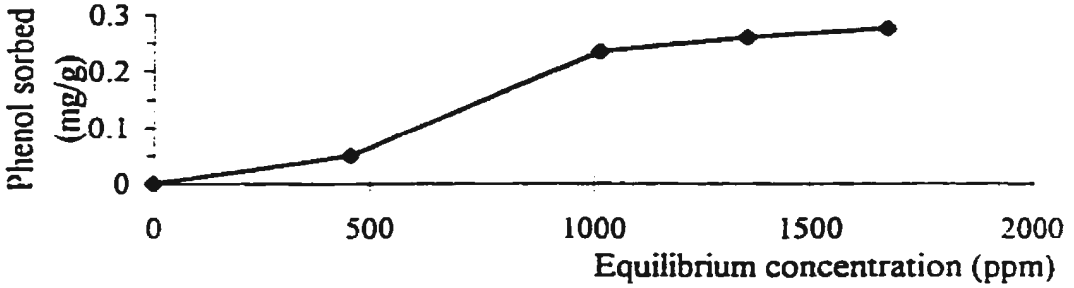

(c) Batch test for CLN with phenol

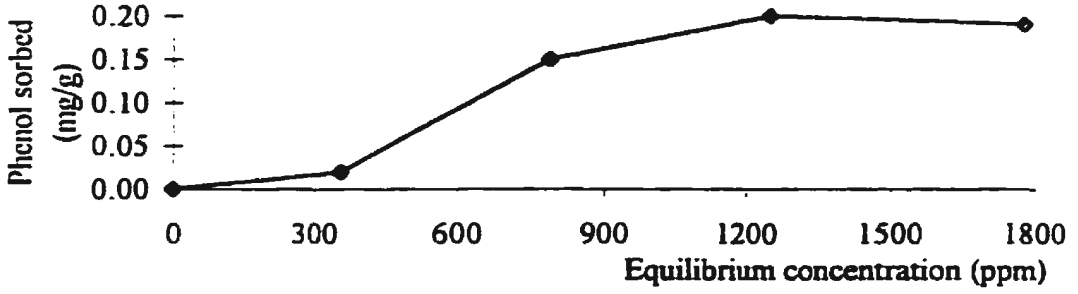

(d) Batch test for NSash with phenol

Figure 5.2 Sorption isotherms from batch tests with phenol

5.3 Hydraulic Conductivity

Hydraulic conductivity (K) is one of the main features observed from column leaching tests. To gain stabilized hydraulic data and complete breakthrough of effluent Pb^{2+}/phenol, each run of the 13 specimens took 6 to 55 days, depending on the material, the compaction of the specimen, the leachate used, and the hydraulic gradient imposed. As shown in Figure 5.3 to 5.5, hydraulic conductivities are plotted as function of pore volume instead of elapsed time. Pore volume is the total volume of a specimen minus the volume of solids. The number of pore volumes is more meaningful than elapsed time, especially when comparing observations of different leaching tests.

Figure 5.3(a) shows the hydraulic conductivity measurements of two pure ashes (i.e. specimen LB-1 and NS-1) and two pure zeolites (i.e. specimen CHB-1 and CLN-1) with leachate-1. For LB-1, NS-1, and CHB-1, their hydraulic conductivities dropped gradually during the first several tens of pore volumes. Eventually, the measurements reached constant values. For CLN-1, the hydraulic process showed a different trend with an initial rising measurement followed by a stabilized hydraulic conductivity. In Figure 5.3(b), 5.4, and 5.5, the trend of initial decline and final stabilization held true between K and pore volume number for the remaining nine specimens. The stabilized hydraulic conductivity values are listed in Table 5.1.

Theoretically, to separate the effects of leachate properties (e.g. viscosity μ and density ρ) from those of the specimen (e.g. the size and the continuity of pore spaces), and make comparable the hydraulic data obtained above, hydraulic conductivities from different synthetic leachates need to be converted to intrinsic permeabilities, i.e. $\frac{K\mu}{\rho g}$.

Solution of $Pb(NO_3)_2$ at 5,000 ppm (i.e. Pb^{2+} at 3125 ppm) at 20°C has kinematic viscosity ($\frac{\mu}{\rho}$) of 1.003 centi-stockes as compared to 1.004 centi-stockes for water at the same temperature (Weast, 1975). Phenol solution with concentration as in leachate-2 and -3 has essentially the μ and ρ values very close to those of water (Environment Canada, 1985). Thus, the differences of kinematic viscosity among leachate-1, -2, and -3 are so small that conversion of hydraulic conductivity to intrinsic permeability seems unnecessary.

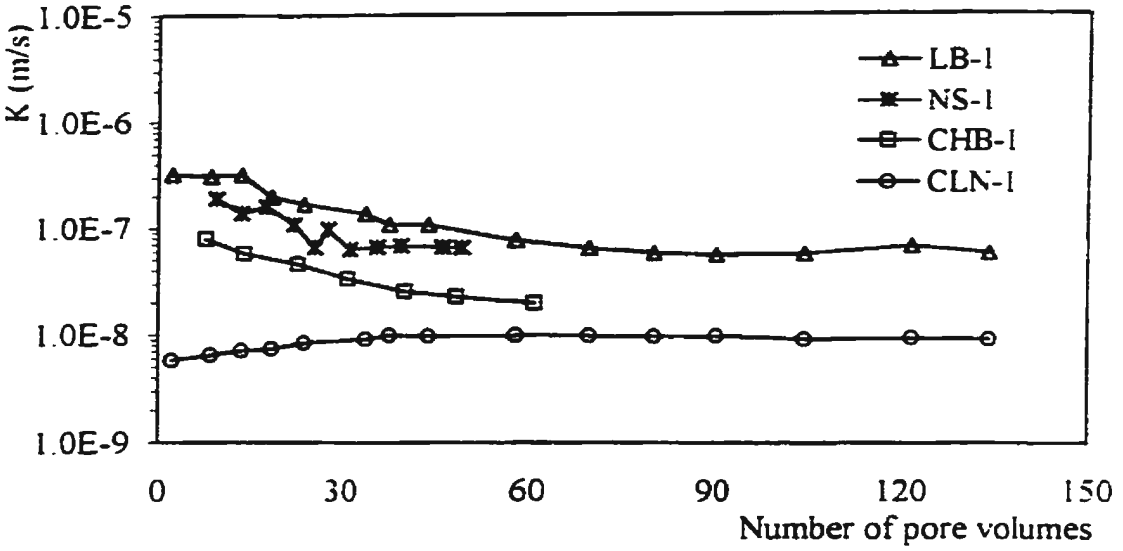

(a) Pure ashes and pure zeolites

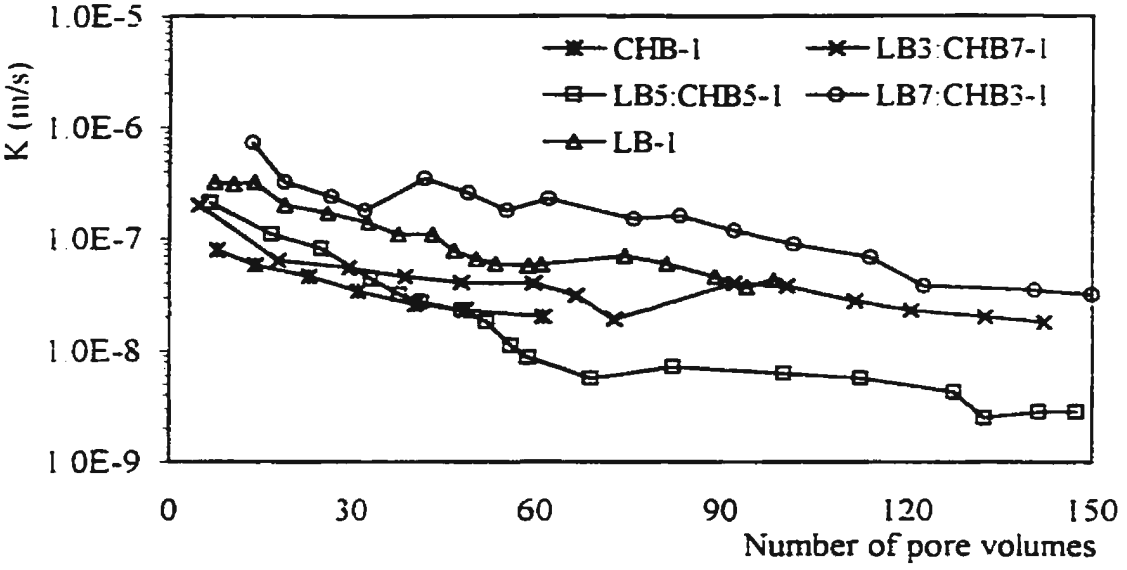

(b) Mixes of CHB and LBash

Figure 5.3 Hydraulic conductivity with Pb^{2-}

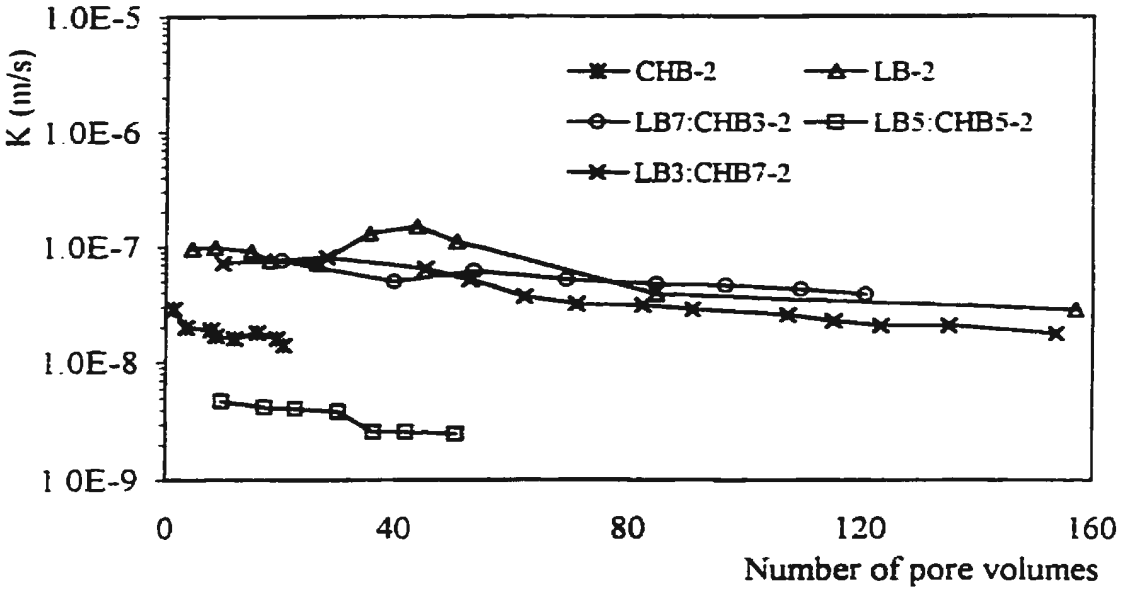

Figure 5.4 Hydraulic conductivity with phenol

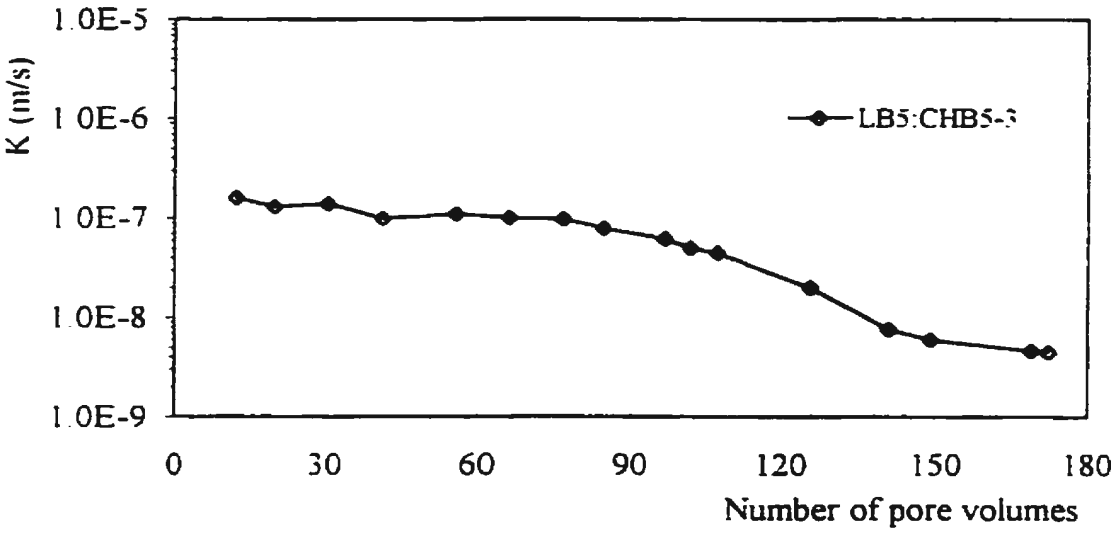

Figure 5.5 Hydraulic conductivity with mixture of Pb/phenol

Table 5.1 Stabilized values of hydraulic conductivity

Specimen I.D.	Leachate	Hydraulic conductivity (m/s)
LB-1	Pb^{2+} = 2500 ppm	7.0×10^{-8}
NS-1		7.0×10^{-8}
CLN-1		1.0×10^{-8}
CHB-1		2.5×10^{-8}
LB3:CHB7-1		2.0×10^{-8}
LB5:CHB5-1		3.0×10^{-9}
LB7:CHB3-1		4.2×10^{-8}
LB-2	Phenol = 55 ppm	3.5×10^{-8}
CHB-2		1.7×10^{-6}
LB3:CHB7-2		2.5×10^{-6}
LB5:CHB5-2		2.5×10^{-5}
LB7:CHB3-2		5.5×10^{-8}
LB5:CHB5-3	Pb^{2+} = 2500 ppm phenol = 55 ppm	4.5×10^{-9}

5.4 Observation of pH

The pH observations during leaching tests on LB5:CHB5-1 and LB5:CHB5-3 are recorded in Figure 5.6. The two profiles are similar with an apparent decline (roughly from pH 10 to pH 8) in the first sixty pore volumes, followed by a quick drop (roughly from pH 8 to pH 6) between the sixtieth and the seventieth pore volume, and a gradual stabilization (pH 5) from after the seventieth pore volume. The pH observation during the leaching test on LB5:CHB5-2 is recorded in Figure 5.7, which shows a gradual decline from pH 9.8 to pH 8.1. The effluent remained basic after LB5:CHB5-2 was leached with 55 pore volumes of leachate-2.

5.5 Pb^{2+} Sorption from Leachate-1

The Pb^{2+} concentrations, C, regularly sampled over time from the effluent solution, are presented as breakthrough curves, in which the ratio, C/C_0, is plotted against the number of pore volumes of effluent discharged, C_0 being the Pb^{2+} concentration in the inflow permeant (i.e. 2500 ppm). Figure 5.8(a) shows the breakthrough curves for pure material specimens, i.e. LB-1, NS-1, CHB-1, and CLN-1. For CHB-1, Pb^{2+} carried in the initial 30 pore volumes of permeant-1 were completely sorbed by the specimen solids. Then Pb^{2+} emerged in the effluent, and Pb^{2+} concentration in the outflow started to rise gradually. The corresponding breakthrough profile extended up to 260 pore volumes, representing the most flat pattern as compared to breakthrough profiles for LB-1, NS-1, and CLN-1. Figure 5.8(b) shows breakthrough curves for LBash-CHB mixture specimens. The higher the chabazite content in a mixture, the flatter its breakthrough curve.

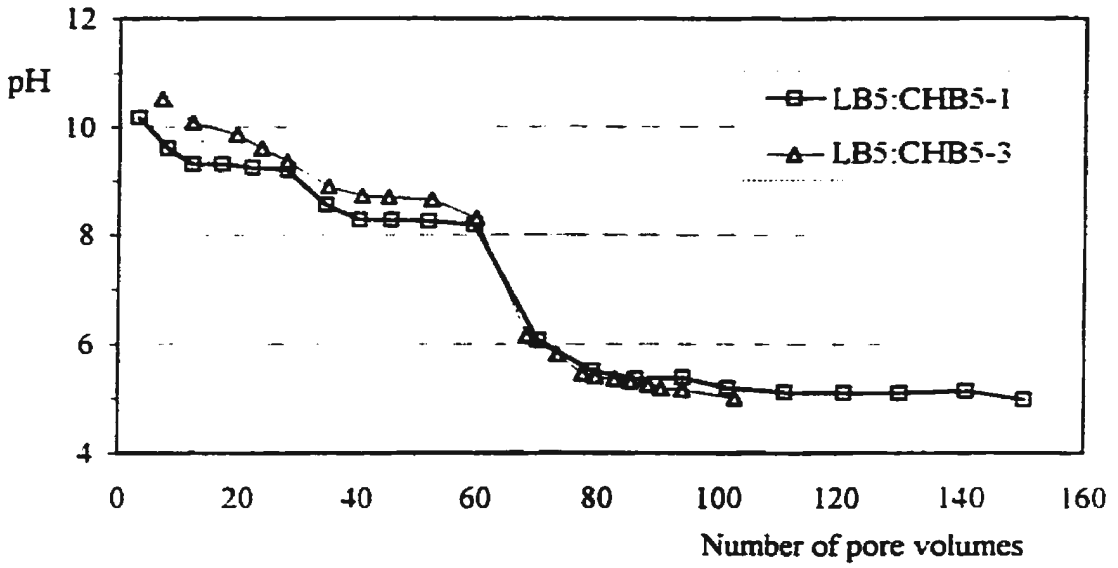

Figure 5.6 The effluent pH with LB5:CHB5-1 and LB5:CHB5-3

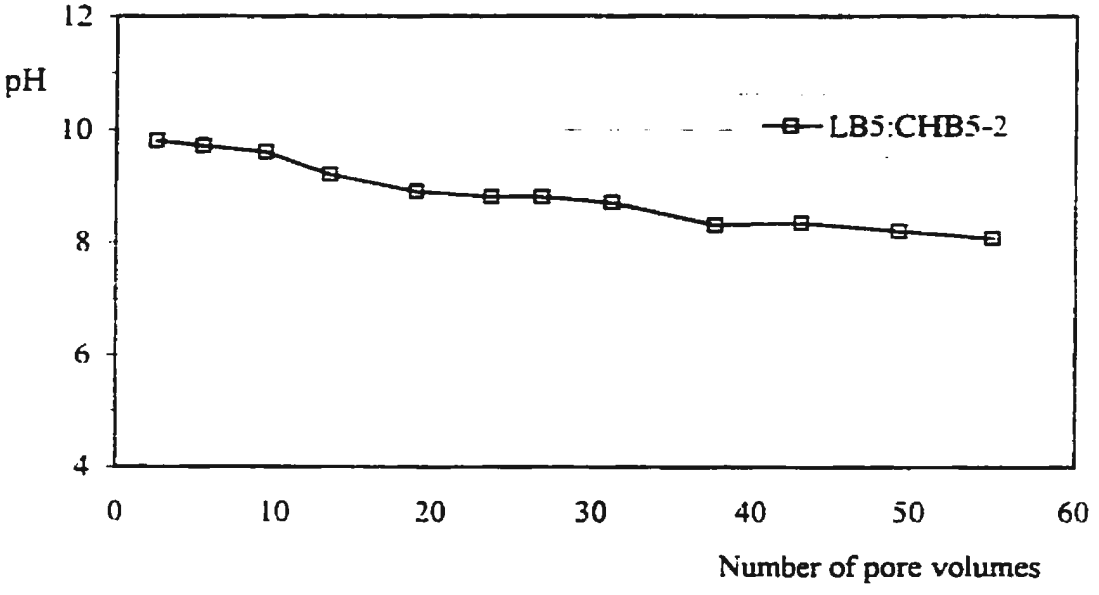

Figure 5.7 The effluent pH with LB5:CHB5-2

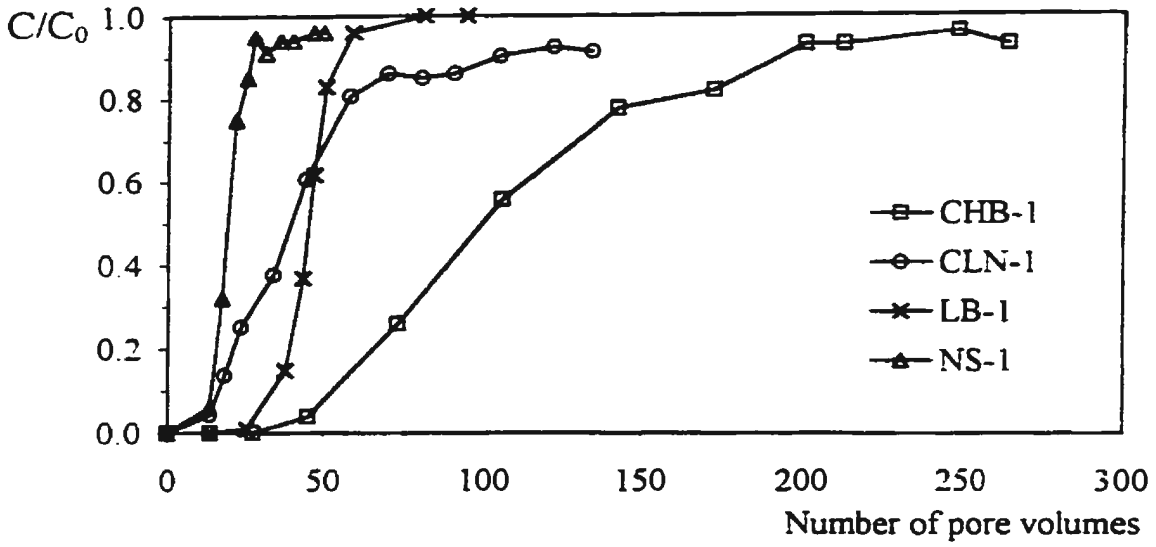

(a) Breakthrough curves for pure materials with Pb^{2-}

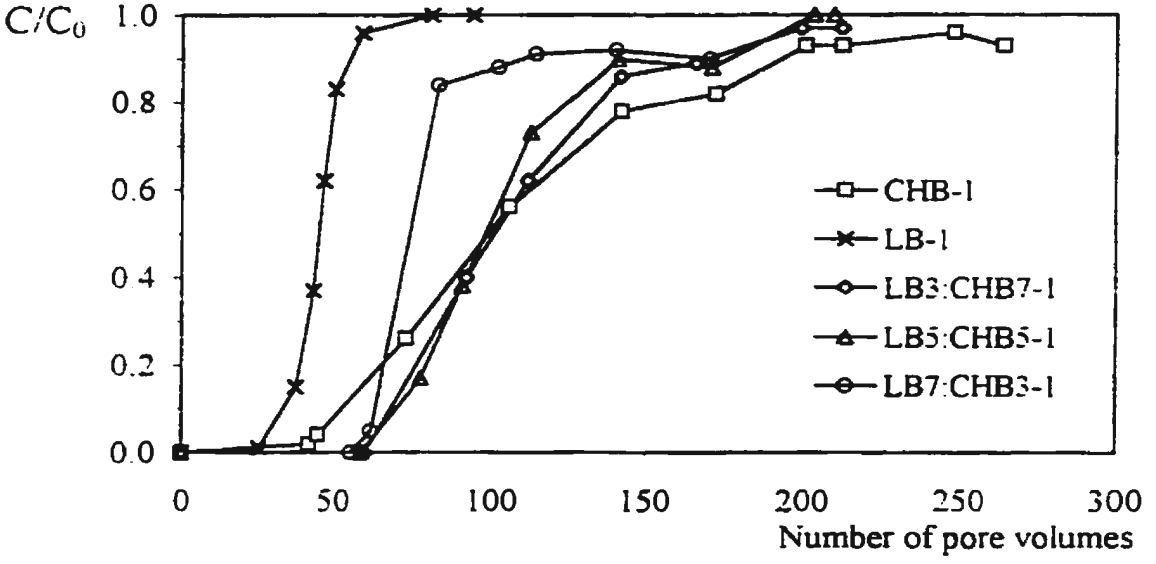

(b) Breakthrough curves for CHB-LBash mixes with Pb^{2-}

Figure 5.8 Breakthrough curves with Pb^{2-}

5.6 Phenol Sorption from Leachate-2

Phenol in leachate-2 was retarded by LBash, CHB, or their mixes as permeant passed through these specimens. For CHB-2, effluent concentration profile exhibited breakthrough behaviour from the start of the leaching test, and reached the concentration plateaued at about 20 pore volumes. LB-2 showed much more potential to attenuate phenol percolation. Its breakthrough curve was so flat as to extend to about 155 pore volumes. The three mixture specimens sorbed more phenol than pure chabazite specimen but less phenol than pure LBash specimen. Hence, their breakthrough curves lies between the curves of CHB-2 and LB-2 (Figure 5.9).

5.7 Pb^{2+} Sorption from Leachate-3

Figure 5.10 is the breakthrough from the leaching test on LB5:CHB5-3. The incoming Pb^{2+} in the initial several ten pore volumes of leachate-3 was completely taken up by LB5:CHB5-3. Then the curve rose fairly quickly and levelled off at about 150 pore volumes. The breakthrough reached its plateau much earlier than in the case of LB5:CHB5-1 that was leached with Pb^{2+} alone. This indicated the occupancy of sorption sites by phenol molecules from leachate-3.

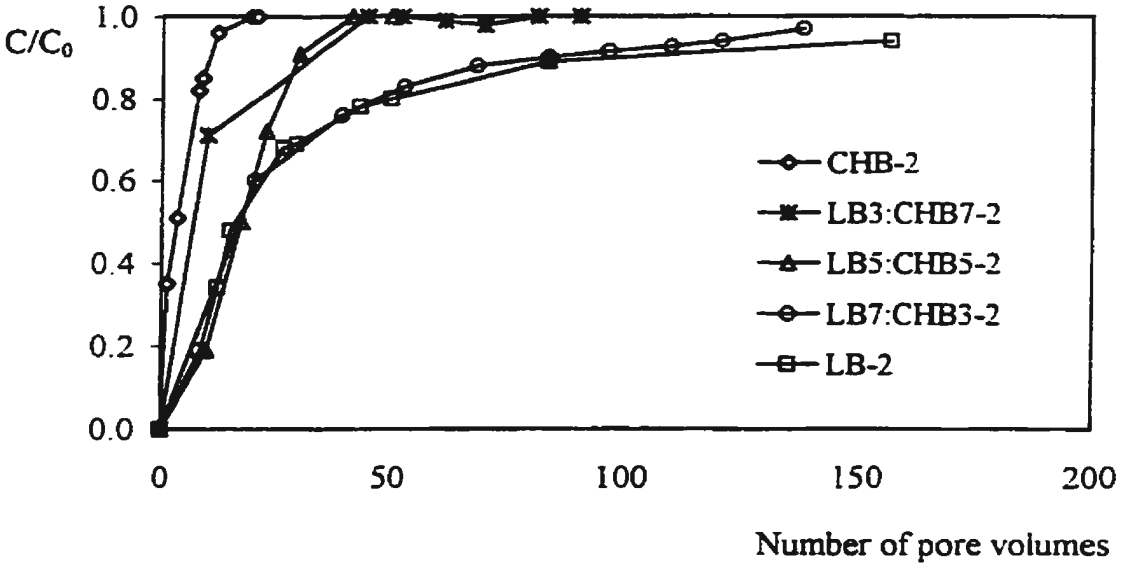

Figure 5.9 Breakthrough curves with phenol

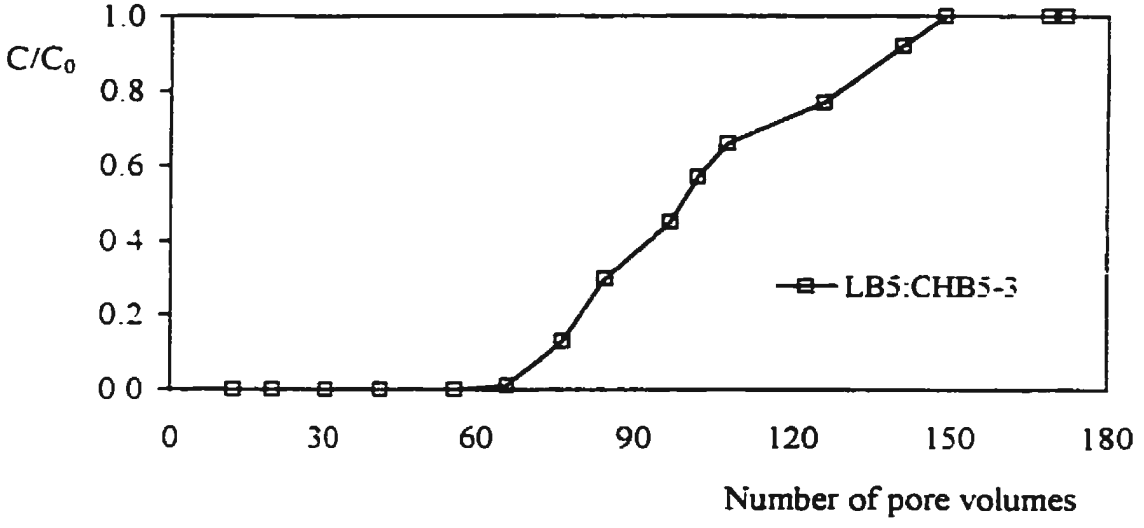

Figure 5.10 Breakthrough curve
with mixture of Pb^{2+}/phenol

6 DISCUSSION

Experimental results are discussed by examining successively the hydraulic conductivity, the Pb^{2+} sorption and partition, the phenol sorption, and the effect of phenol on Pb^{2+} sorption.

6.1 Hydraulic Property

Hydraulic conductivity of a solid specimen mainly depends on the solid properties, specimen compaction, degree of saturation, and permeant chemistry.

6.1.1 Hydration Effect

In LBash and NSash, the principal constituent is SiO_2, which accounts for 43% by weight for both ashes. Like quartz sand, SiO_2 has no swelling tendency in the presence of moisture, and remains relatively inert. Other major mineral crystallines, such as mullite, and magnetite, are not appreciably reactive with respect to water. As far as fly ash hydration is concerned, the most reactive species in ordinary fly ash is lime (CaO). A portion of the overall analytical CaO content is present as crystalline CaO (Roy et al, 1985). Individual CaO crystalline particles are either embedded within the glass or deposited as a film on its surface. The CaO on glass surface is more likely to dissolve into water, and yields $Ca(OH)_2$, a cementing product. Usually, this reaction is relatively slow. Hydration may also happen to MgO, which exists in small amount in fly ash as periclase crystal or soluble oxide in glass. Formation of $Mg(OH)_2$ also contributes to join ash particles. In addition, products from hydration reactions may include calcium

hydrosilicate ($3CaO{\cdot}2SiO_2{\cdot}3H_2O$) and ettringite ($3CaO{\cdot}Al_2O_3{\cdot}3CaSO_4{\cdot}Al_2O_3{\cdot}32H_2O$), both being colloidal precipitates that bridge the glass spheres. Cementing compounds from the hydration of high calcium fly ashes significantly limit the permeability of ash specimens. However, as type F fly ash, LBash and NSash only have low CaO contents and possess little self-cementing value. In the compacted specimens, like NS-1 and LB-1, no enough cementing agent exists to bind silica particles. Consequently, they are as permeable as 7×10^{-8} m/s, in agreement with the measurement made by Ontario Hydro on their local fly ash (Chan, 1991). Also, the unburnt carbon particles are relatively inert in hydration reactions. Carbon fragments act as a diluent that attenuates the cementing ability of the fly ash, and favours the increase in the permeability of fly ash (Roy et al, 1985).

The hydraulic behaviour of natural zeolites, like chabazite and clinoptilolite, can be attributed largely to their geological origins. Most natural zeolites in sedimentary rocks were formed from finely-grained volcanic ash. After deposition, the noncrystalline volcanic ash hydrated and reacted with pervading lake, marine, or groundwater, probably by a dissolution-reprecipitation mechanism, and transformed into micrometer-size crystals of zeolites. In the crushed bulk natural zeolite samples, such as the ones used in this study, the impurity mineral particles are mainly in the micrometer size range, filling pore spaces in the powder ore. As hydrated aluminosilicates, zeolites can lose or gain water reversibly without major change of structure. Loosely bound molecular water surrounds the exchangeable cations in the pore spaces of zeolite framework, but only large three-dimensional cavities are passageways of free water, which contributes to material permeability and the migration of inorganic cations.

The intense hydration reactions can be reflected by the sorption heat that accompanies zeolite hydration. The adsorption heat (12~13 kcal/mol zeolite) is higher than the liquefaction heat of water (10 kcal/mole, Flanigen, 1983). In fact, significant heat build-up was observed during specimen preparation for CLN-1, CHB-1, and CHB-2. The observed heat should include the hydration heat from the dissolution of lime (CaO). The temperature of zeolite specimens increased, and the dissolution of other soluble matters was promoted. Cementation compounds, such as calcium hydroxide, calcium aluminate hydrate, and calcium silicate hydrate, could be expected as reaction products, which aggregate zeolite solids and reduce the specimen hydraulic conductivity to about 2×10^{-6} m/s.

Comparatively, in the two fly ashes, 78% to 85% (by weight) of grains are under silt size (< 0.074 mm); in the two zeolites, 0 to 10% of the grains are under silt size (Figure 3.1). However, CLN and CHB exhibited stronger hydration and stronger cementitious characteristics than LBash and NSash. The zeolite specimens showed smaller hydraulic conductivity values than the fly ash specimens.

6.1.2 Behaviour of Mixture Materials

When LBash is mixed with CHB, the extremely fine size of ash particles and their spherical shapes allow good filling of voids between zeolite particles, which substantially reduces the porosity of a mixture specimen. In the compacted specimen at nearly optimum water content, LBash and CHB particles fit each other tightly. The two pozzolanic materials chemically react with calcium hydroxide and other cementitious agents, and lead to a hydraulic conductivity slightly less than the values of pure zeolite specimens. The measurement on specimens of various CHB/LBash ratios showed a non-monotonic trend between material proportion and specimen hydraulic conductivity. That is, the more LBash in the mixture, the less voids but less cementitious binder formed in the specimen; conversely, the more CHB, the more cementitious binder but more voids expected instead. The trend existed in leaching tests with leachate-1 and leachate-2, as is illustrated in Figure 6.1. It can be seen that 50% LBash with 50% CHB appeared a compromising proportion which possessed limited porosity and adequate cementation to form a specimen with minimum hydraulic conductivity. A mixture specimen at this proportion is likely to show the best hydraulic performance in liner application.

6.1.3 Permeant Effect

Conceptually, if an inorganic solution is used as permeant in lieu of water, ion exchange takes place and the thicknesses of diffuse double layer (DDL) around specimen particles may be altered. The DDL concept will be described further in Section 6.2.1, while its thickness, H, is given herein (Michell 1993), i.e.

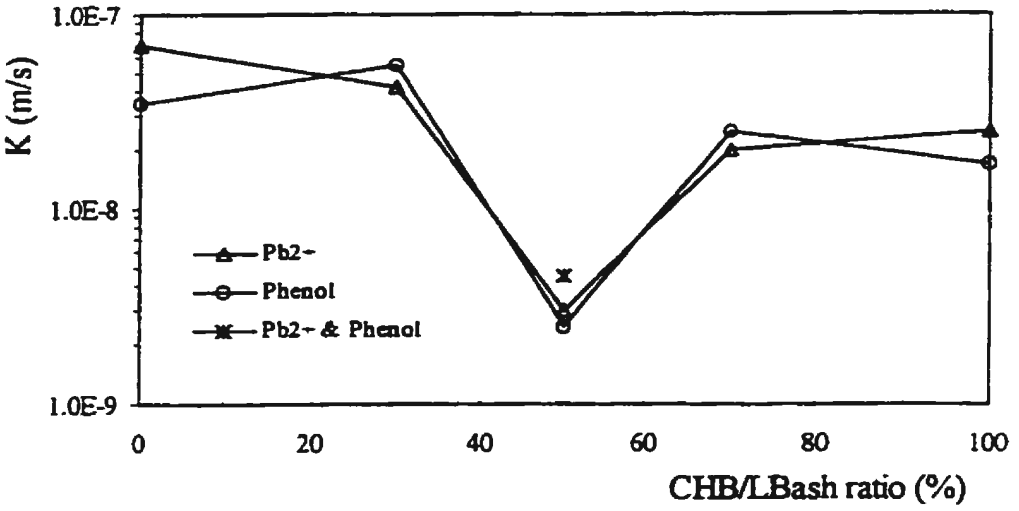

Figure 6.1 Hydraulic conductivity versus CHB/LBash ratio

$$H = \left[\frac{DBT}{8\pi n_0 \epsilon^2 v_a^2}\right]^{1/2} \qquad (6.1)$$

where D = dielectric constant of the pore fluid; B = Boltzman constant; T = temperature (°K), n_0 = electrolyte concentration of the pore liquid; ϵ = unit electric charge; v_a = valence of cations in the pore liquid. Eq. (6.1) suggests that replacement of host monovalent cations with multivalent guest cations can cause the reduction in DDL thickness and thus the increase of repulsive force between solid particles. The fabric of the test specimen becomes more flocculated with larger pore spaces, making the specimen more permeable. But on the other hand, metal ions in the inorganic permeant often form hydroxide precipitation with resulting blockage of pore spaces and decreases in hydraulic conductivity. The two mechanisms (i.e. fabric flocculation and metal precipitation) may

occur simultaneously to both fly ash and zeolite when they are leached with inorganic permeant. Probably, the combined effect of inorganic leachate on the hydraulic conductivity of a mixture specimen is not significant, as reported by Peirce (1984) with clay liner and by Edil et al (1992) with compacted fly ash.

The permeant effect of phenol usually depends on the concentration of the solution. High-strength phenol solution may give an increased hydraulic conductivity, but low-strength phenol solution (e.g. less than 950 ppm) has no apparent effect on the hydraulic conductivity of a clay specimen (Goldman et al, 1990).

6.2 Pb^{2+} Sorption

In the previous text, sorption has been used as a general term to bracket all the processes by which Pb^{2+}/phenol are withdrawn from leachate solution and sorbed to fly ash or zeolite solids. The actual processes in a sorbate-sorbent system include physical adsorption (physisorption), chemical adsorption (chemisorption), complex formation, and precipitation. Ionic sieving is also an important action that characterizes the Pb^{2+} sorption onto zeolite. All these processes occur simultaneously with a relative importance, depending on the local chemical environment.

6.2.1 Physisorption of Pb^{2+}

Physisorption of Pb^{2+} occurs primarily as a result of electrostatic interaction. Oxide and silicate surfaces of fly ash and zeolite generally consist of closely packed oxygen lattices. Over the solid surface there are residual negative electrostatic charges,

which are originated from the isomorphic substitution of Al^{3+} or Fe^{3+} for Si^{4+} in tetrahedral layers and of Fe^{2+} or Mg^{2+} for Al^{3+} in octahedral layers. More intense sites of negative charge exist on the surface layer where there are lattice imperfections. When a fly ash/zeolite specimen is presoaked with water for initial saturation in a leaching test, on the solid surface of the aqueous system accumulates an immobile monolayer of water molecules that are tightly bound to the surface. Outside the immobile layer is an accumulation of cations (i.e. K^+, Na^+, Ca^{2+}, and Mg^{2+}) which are dissociated from fly ash or zeolite solids with electrical charges opposite that of the surface and which are therefore called counter-ions. The electrostatic interaction between surface charge and counter-ions reaches equilibrium with minimum free energy. Counter-ions diffusively distribute with decreasing concentration away from the solid-liquid interface, thus establishing a "diffuse double layer" (DDL) of ions in the vicinity of the interface. When Pb^{2+} permeant is introduced into the ash/zeolite specimen, the pore fluid becomes a mixed "electrolyte solution". Pb^{2+} and counter-ions start to compete for sorption or exchange sites. The selectivity of the zeolite and fly ash exchanger for Pb^{2+} and the counter-ions is mainly controlled by properties of these ions (i.e. valence, ionic radius, and individual concentration) and the exchangers (i.e. exchange sites and pore sizes). Maintaining Pb^{2+} concentration at a "concentrated" level (like 2500 ppm in leachate-1 and -3) can definitely favour its competitive power, while counter-ions are continuously attenuated by permeant entrainment. Consequently, Pb^{2+} ions succeed in replacing the localized counter-ions from the solid-liquid interface, and become attached there. This type of sorption process is commonly described as cation exchange, and schematically represented by

$$\equiv S\text{-[Counter-ions]} + Pb^{2+} \longleftrightarrow \equiv S\text{-Pb} + \text{[counter-ions]} \qquad (6.2)$$

where $\equiv S$ refers to ash/zeolite particles. Eq. (6.2) must be a stoichiometric process because of the preservation of the system electroneutrality, or an equivalent amount of charges has to transfer at the liquid-solid interface. As a result of the reaction, the immobile monolayer adjacent to the interface, the so-called Stern layer, accumulates Pb^{2+} ions at highly charged sites. Such ions are held at molecular distance from the solid surface. The retention of Pb^{2+} ions in the Stern layer depends on the electrostatic force (non-functional group) at negatively charged sites, the relative concentration of Pb^{2+} in the bulk solution, and the dehydration energy of the counter-ions. The transition zone in the DDL, or "Gouy layer", varies in its thickness with the surface charge of the solid, ionic strength, and dielectric constant of the liquid phase (see Eq. (6.1)).

In the early stage of the reaction in Eq. (6.2), there are excessive counter-ions (K^+, Na^+, Ca^{2+}, and Mg^{2+}) but inadequate $\equiv S$-Pb^{2+} bound to specimen solid. The cation exchange reaction proceeds toward the formation of $\equiv S$-Pb species. Accordingly, the rate of Pb^{2+} exchanging in the early stage of a leaching test is close to or even exceeds the rate of Pb^{2+} supply from permeant. Hence, the incoming Pb^{2+} ions are depleted from pore liquid with other co-existing processes like Pb^{2+} complexation and precipitation that are involved to certain extent. Although a significant gradient of Pb^{2+} concentration exists between the solid surface and the bulk pore liquid, electrostatic interaction in the DDL prevents Pb^{2+} ions from free diffusion toward bulk solution. The Pb^{2+} depletion in the early leaching stage is reflected in Figure 5.8, where specimens of pure LBash, pure CHB,

or their mixes were percolated with leachate-1, but no outgoing Pb^{2+} was measurable in the first several ten pore volumes of effluent. As the cation exchange reaction progresses, more and more counter-ions on solid surface are replaced and eventually leached out into the effluent. $\equiv S$-Pb species accumulates at sorbent surface. The rate of the forward reaction in Eq. (6.2) gradually slows down, so an increasing number of Pb^{2+} ions from the permeant supply at a constant concentration remain unattracted onto the DDL. Finally, the accumulation of $\equiv S$-Pb species grows to such a level at which cation exchange reaction in Eq. (6.2) reaches equilibration, and the effective cation exchange capacity of the ash/zeolite solids is fully exhausted. Subsequent Pb^{2+} ions added by permeant inflow are likely to participate in other reactions or escape into effluent.

6.2.2 Chemisorption of Pb^{2+}

Dissimilar to the physisorption through which sorbent-sorbate interface undergoes no permanent chemical alteration, chemisorption involves short-range chemical valence bonds, and may yield a sorbed layer with properties very different from those of the original surface. To make an easy description of chemisorption phenomena, a schematic cross section of zeolite (or fly ash) surface layer is depicted in Figure 6.2(a). It clearly shows that, because of an excess of surface negative charges around zeolite and fly ash solids, the metal ions over the outer surface have a smaller coordination number (the number of neighbour anions bonded to the current central metal ion in the structure) than those in the inner layers, and thus behave as Lewis acids (which can accept a pair of electrons to form a new bond). In hydrated conditions, the exposed metal cations tend

to coordinate water molecules (Figure 6.2(b)). A hydroxylated surface is formed through dissociative chemisorption (Figure 6.2(c)). Generally, hydroxylation of SiO_2 is a slow process whereas the -OH groups on Al_2O_3 and Fe_2O_3 species are formed rapidly. The number of -OH groups per $100Å^2$ ranges between 4 and 10 on ordinary oxide surfaces (Schindler, 1981). In Figure 6.2(c), there are two different types of -OH groups: type I being terminal hydroxyl bond to one metal ion; and type II being hydroxyl bridged to two or more metal ions. In Figure 6.3(a), IR spectroscopy has offered evidence for the two -OH types present in chabazite framework. The terminal hydroxyls reside at 3740 cm^{-1}. They are not polarized by neighbouring Al (Figure 6.3(b)), and have a weak acid strength. The bridged hydroxyls reside between 3650 and 3500 cm^{-1}, and are polarized by the neighbouring Al tetrahedra (Figure 6.3 (a) and (c)) with a strong acid strength.

After the hydration and hydroxylation of zeolite and fly ash, three surface species appear: $\equiv S\text{-}OH$, $\equiv S\text{-}O^-$, and $\equiv S\text{-}OH_2^+$ (Morel et al, 1981).

$$\equiv S\text{-}O^- + H^+ \Leftrightarrow \equiv S\text{-}OH \qquad (6.3)$$

$$\equiv S\text{-}OH + H^+ \Leftrightarrow \equiv S\text{-}OH_2^+ \qquad (6.4)$$

The probable chemisorption of surface species with Pb^{2+} may occur as follows

$$\equiv S\text{-}OH + Pb^{2+} \Leftrightarrow \equiv S\text{-}O\text{-}Pb^+ + H^+ \qquad (6.5)$$

$$\begin{matrix} \equiv S-OH \\ \equiv S-OH \end{matrix} + Pb^{2+} \Leftrightarrow \begin{matrix} \equiv S-O \\ \equiv S-O \end{matrix}\!\!>\!Pb + 2H^+ \qquad (6.6)$$

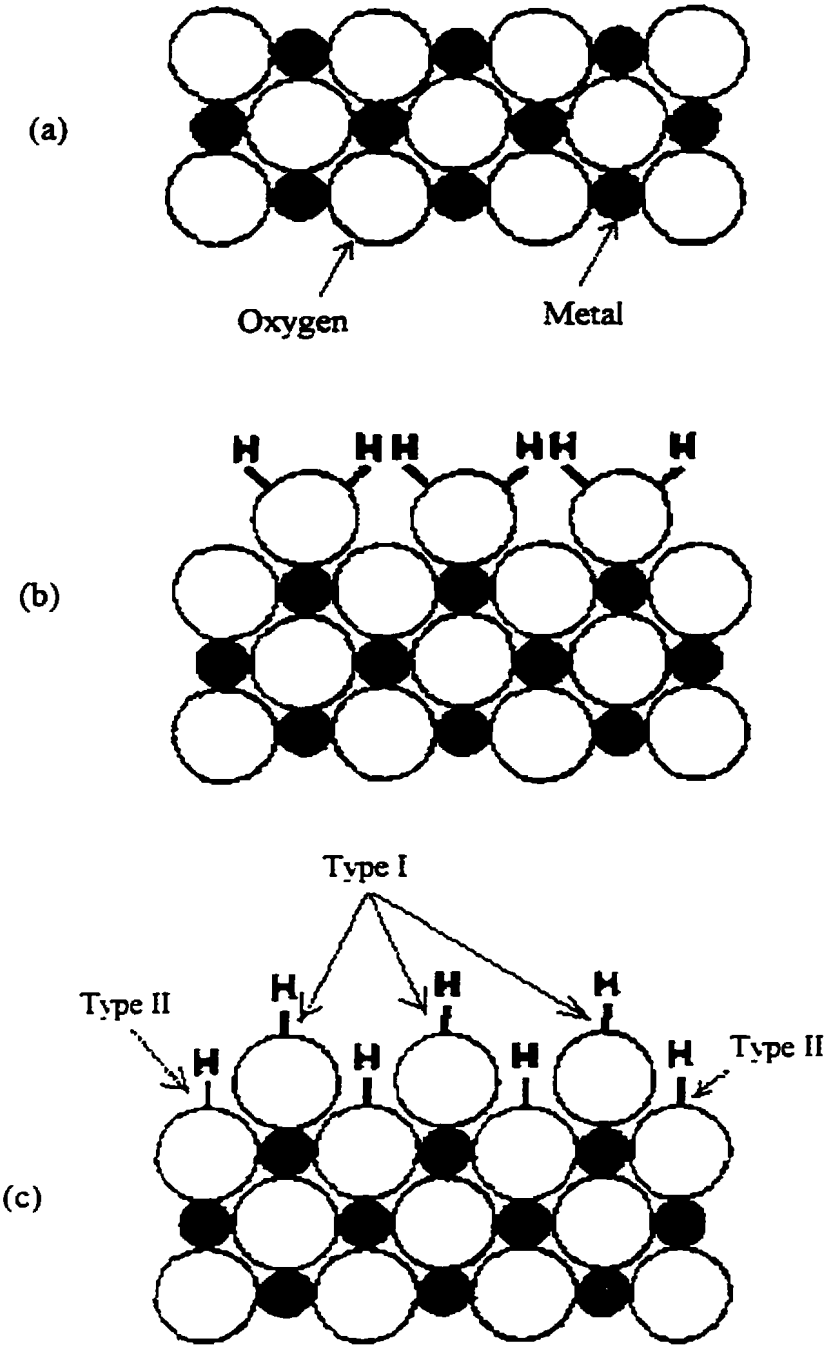

(a) Surface ions coordinatively unsaturated
(b) Coordination of surface ions with H_2O molecules
(c) Hydroxylated surface

Figure 6.2 Cross section of the surface layer of a metal oxide (Schindle 1981)

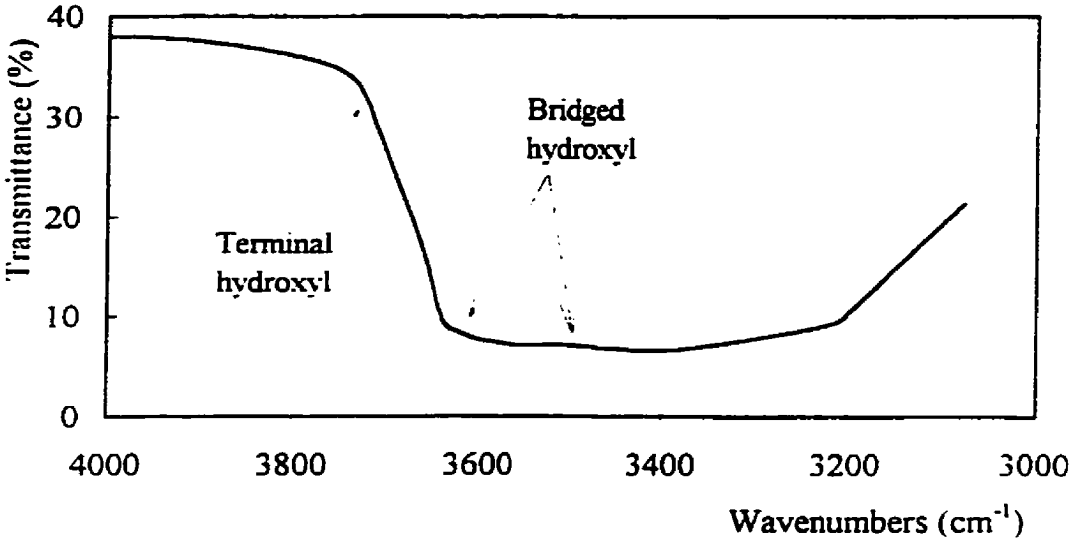

(a) Infrared spectrum for CHB showing hydroxyl types

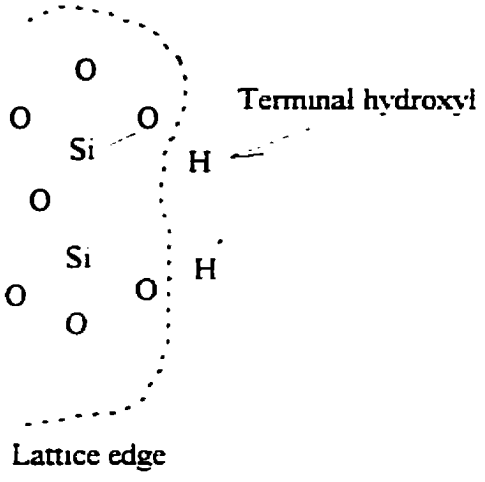

(b) Terminal hydroxyl

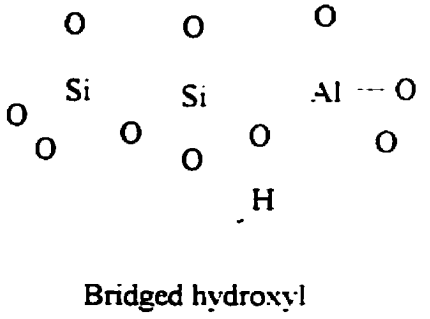

(c) Bridged hydroxyl

Figure 6.3 Two types of hydroxyls in chabazite framework

$$\equiv\mathcal{S}\text{-}OH_2^+ + Pb^{2+} \Leftrightarrow \equiv\mathcal{S}\text{-}O\text{-}Pb^+ + 2H^+ \quad (6.7)$$

$$\equiv\mathcal{S}\text{-}OH_2^+ + Pb^{2+} \Leftrightarrow \equiv\mathcal{S}\text{-}OHPb^{2+} + H^+ \quad (6.8)$$

$$\equiv\mathcal{S}\text{-}OH_2^+ + Pb^{2+} + H_2O \Leftrightarrow \equiv\mathcal{S}\text{-}OPbOH + 3H^+ \quad (6.9)$$

These reactions are not equally favourable depending on variables like the acid-base chemistry of surface hydroxyl groups, the pH of the bulk liquid, the Pb^{2+} concentration, and the extent to which the surface sites are being saturated.

6.2.3 Pb^{2+} Complexation

Complexation is another speciation process related to Pb^{2+} sorption by zeolite and fly ash. It occurs when Pb^{2+} reacts with various inorganic or organic ligands. Inorganic ligands include anions such as OH^-, CO_3^{2-}, HCO_3^-, and Cl^-, but OH^- is the predominant ligand with zeolite and fly ash. Organic ligand in the present experimental system refers to carboxyl ions ($-COO^-$) with LBash. Complexes are of two types in terms of the distance between complex unit and the surface site, namely, inner sphere complex and outer sphere complex.

Inner sphere complexes are in direct contact with surface, and readily contribute to Pb^{2+} sorption. The pertinent equilibria for inner sphere complex formation can be written

$$n\cdot \equiv\mathcal{S}\text{-}OH + Pb^{2+} + L \Leftrightarrow (\equiv\mathcal{S}\text{-}O)_n\text{-}Pb\text{-}L^{(2-n)+} + n\cdot H^+ \quad (6.10)$$

$$n\cdot \equiv\mathcal{S}\text{-}OH + L + Pb^{2+} \Leftrightarrow (\equiv\mathcal{S})_n\text{-}L\text{-}Pb^{(2+n)+} + n\cdot OH^- \quad (6.11)$$

where n = 1 or 2; L is a ligand.

Outer sphere complexes are formed apart from the solid-liquid interface. In such complexes, ligands (or anions like OH^-) tend to increase aqueous Pb^{2+} concentration by binding aqueous Pb^{2+}, keeping it in pore solution, but preventing it from taking part in physisorption or chemisorption that would otherwise reduce its concentration. Outer sphere complexes may be monomeric or polymeric. Monomeric hydroxy complexes appear as $PbOH^+$, $Pb(OH)_3^-$, and/or $Pb(OH)_4^{2-}$. The latter two complexes are significant only above pH 7, which is the case in the early stage of the leaching tests with LB5:CHB5-1 and LB5:CHB5-3 (see Figure 5.6). As a cation, $PbOH^+$ is more likely to be sorbed to a negatively charged surface than are the anions $Pb(OH)_3^-$ and $Pb(OH)_4^{2-}$. Polymeric hydroxide complexes are formed at a rather high aqueous Pb^{2+} concentration with definite structural patterns. They are dominant between pH 6.0 and 10.0 only when Pb^{2+} concentration exceeds 0.1 molar (20,700 ppm). Only monomers are significant if total dissolved Pb^{2+} is less than 10^{-5} molar (2.07 ppm) (Brow and Hem, 1984). Since the Pb^{2+} concentrations in the present synthetic leachates are between 0.1 and 10^{-5} molar, the significance may be alike for both monomeric and polymeric complexes. Pb^{2+} ions bonded within polymeric complexes are more stable, or less likely to be sorbed, than those bound within monomeric complexes.

In LBash, the organic component has a high affinity for Pb^{2+} ions because of the strong ligands furnished by carboxyl ions ($-COO^-$). The carboxyl ion is derived from the ionization of carboxyl group -COOH, i.e.

$$R\text{-}COOH + H_2O \Leftrightarrow R\text{-}COO^- + H_3O^+ \qquad (6.12)$$

where R represents a carbon framework. With increasing pH, the Pb^{2+} complex is likely

to be more stable due to the increased ionization of the functional group, and Pb^{2+} chelation is thus induced. By and large, the complex formed between Pb^{2+} ions and organic ligands are much stronger than those formed with inorganic ligands.

6.2.4 Pb^{2+} Precipitation

Distinguished from the physisorption, chemisorption, and complexation, precipitation plays an important role in Pb^{2+} sorption. It occurs mainly as $Pb(OH)_2$ because of its low solubility product, i.e. $K_s=10^{-15.1}$. The process includes two stages: nucleation and particle growth. When leachate Pb^{2+} concentration exceeds the critical supersaturation with respect to K_s, nucleation takes place on zeolite and fly ash surface or even in the pore liquid. The precipitated substance accumulates from constant Pb^{2+} supply at the suitable pH in the system. The pH of the pore fluid in test specimens is an important factor to control precipitation. At either low pH or very high pH, $Pb(OH)_2$ shows rather high solubility so that no precipitation is expected. Within a range of fairly high pH values, e.g. pH = 8 ~ 10 as observed in the leaching test with LB5:CHB5-1 and LB5:CHB5-3 (see Figure 5.6), $Pb(OH)_2$ shows very low solubility, and precipitates constitute a significant part of Pb^{2+} retardation.

6.2.5 Ionic Sieving

Ionic sieving is a unique feature of zeolite. It is necessary to have a deep insight into the zeolite crystal structure before understanding the Pb^{2+} removal through this mechanism. In Figure 6.4, a basic structural unit of chabazite framework is outlined as

a rhombohedral cell joined with two pseudo-hexagonal prisms. At the corners of the hexagonal prisms lie Si, Al atoms, while oxygen atoms lie between each pair of Si, Al atoms. Figure 6.4(a) is a simplified model omitting the deformation of hexagonal prisms. Figure 6.4(b) shows the link between adjacent units with a true representation of the pseudo-hexagonal prisms. The centre of each pseudo-hexagonal prism is at the corner of the rhombohedral cell. Six of the cell faces are rhombohedral, each containing one aperture, through which molecules and ions can pass into the inside cavity.

Figure 6.5(a) is a projection down the y-axis of the chabazite polyhedron unit. Si, Al atoms (solid circles) and oxygen atoms (open circles) are bound to form tetrahedra. In the centre of Figure 6.5(a) is an aperture, which has free dimensions of 3.7×4.2Å (Figure 6.5(b)). Parallel aperture windows on adjacent polyhedrons are shown in Figure 6.5(b). These apertures provide incoming Pb^{2+} ions (1.32Å of ionic radius) with numerous pathways towards the larger cavity (i.e. micropores), where Pb^{2+} ions are trapped securely.

The internal sites are so numerous with honeycombed chabazite, as manifested in Figure 6.4~6.5, that the ionic sieving becomes a valuable quality for Pb^{2+} sorption on a zeolite/ash mix.

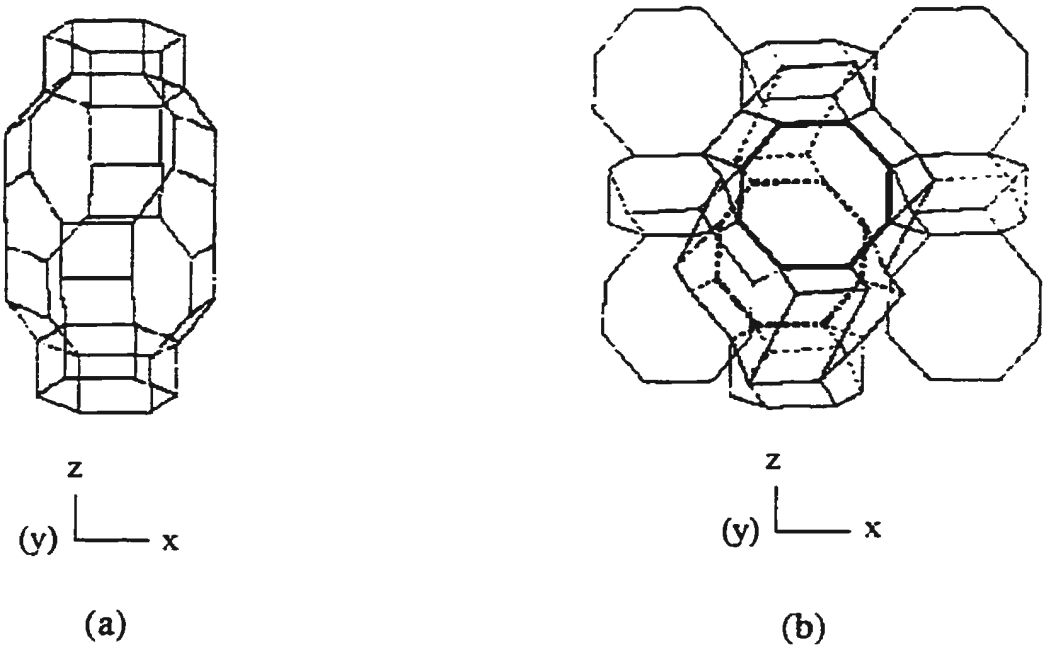

Figure 6.4 Three dimensional pattern of chabazite framework (Berrer et al 1959)

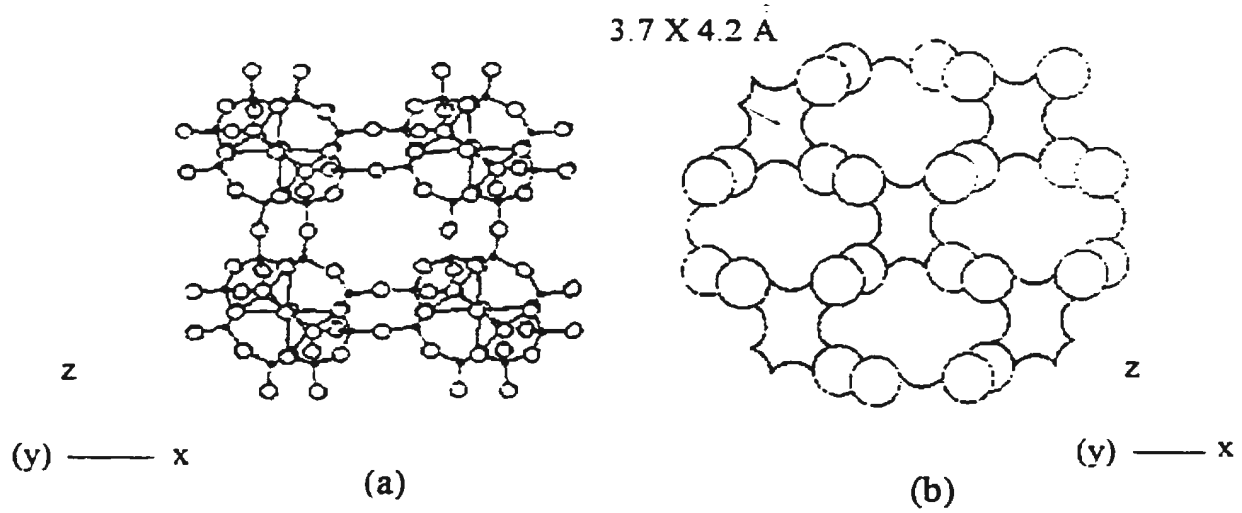

Figure 6.5 Structural aperture of chabazite framework

6.2.6 Pb^{2+} Sorption Capacity

Based on the mass balance principle, the amount of Pb^{2+} sorbed on each Pb-saturated specimen, T_{pb}, was determined by subtracting the Pb^{2+} output from Pb^{2+} input of the pertinent leaching test. For comparison, T_{pb} is expressed as total sorbed Pb^{2+} per gram of specimen solid (mg/g), i.e.

$$T_{pb}=\frac{1}{M_s}\sum_{i=1}^{n} C_0\left(1-\frac{C_i}{C_0}\right)V_i \qquad (6.13)$$

where C_0 = 2500 ppm; M_s is the mass of the specimen solids; C_i/C_0 is the relative concentration at i_{th} pore volume of the corresponding breakthrough curve; V_i is the effluent volume collected during the i_{th} time interval. The individual T_{pb} values determined according to Eq. (6.13) for all the specimens with leachate-1 are illustrated in Figure 6.6. Among pure material specimens, CHB-1 retained 4, 4.5, or 21.7 times as much Pb^{2+} as did LB-1, CLN-1, or NS-1, respectively. LB-1 retained slightly more Pb^{2+} than CLN-1. The difference in Pb^{2+} sorption among the four materials is consistent with the trend of their sorption isotherms identified via batch tests (Figure 5.1).

6.2.7 CHB/LBash Ratio versus Pb^{2+} Sorption

For mixture specimens constructed with LBash and CHB, CHB is more responsible for Pb^{2+} retention. Figure 6.7 shows that their sorption capacities are proportional to the CHB content.

The capacity of Pb^{2+} sorption, however, is not the only criterion in designing the best recipe of composite liner materials. Other properties, such as hydraulic conductivity and the capacity to retain organic leachate, should also be taken into account.

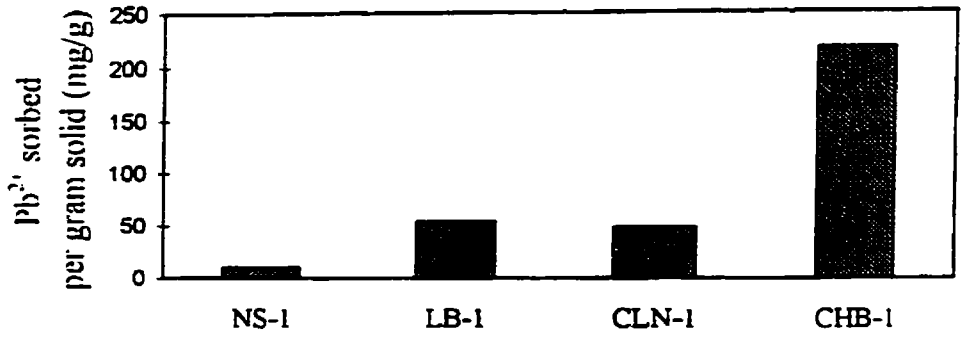

(a) For pure materials

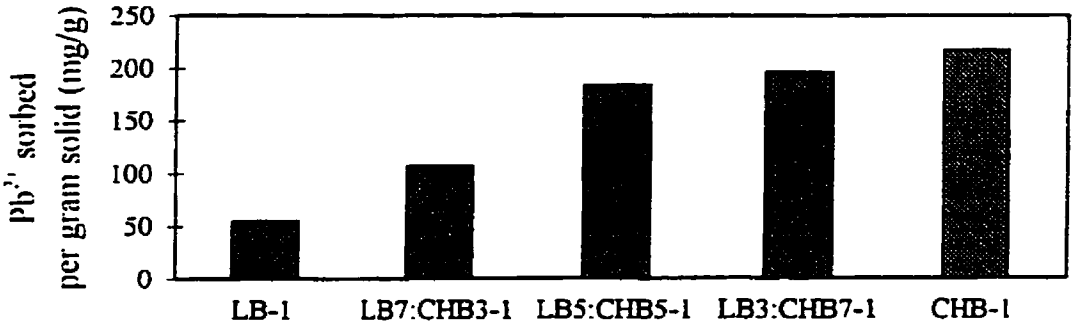

(b) For CHB-LBash mixes

Figure 6.6 The amount of Pb^{2+} sorbed on each test specimen

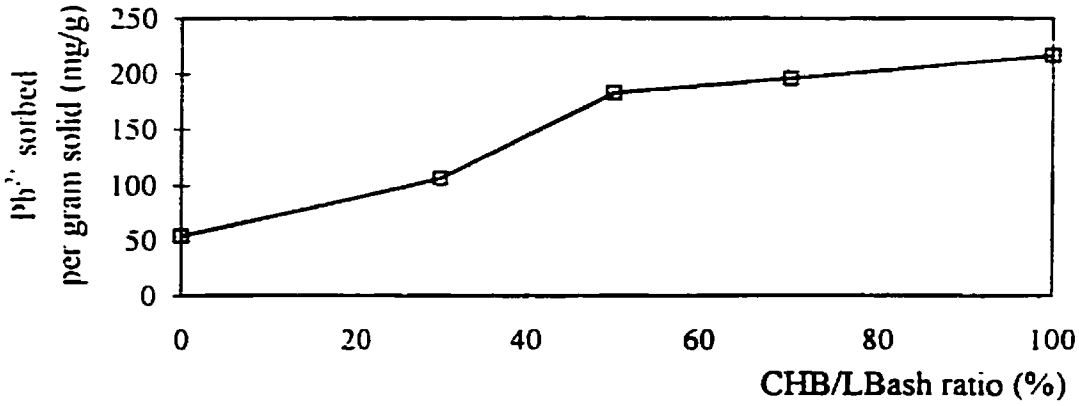

Figure 6.7 Pb^{2+} sorption capacity versus CHB/LBash ratio

6.2.8 Partition of Pb^{2+} Sorption

Section 6.2.1 to 6.2.5 qualitatively described reactions concerning Pb^{2+} sorption. Discussion in this section will be addressed more quantitatively to the partitioning of sorbed Pb^{2+} among four fractions. As mentioned in Section 4.3.4, the four fractions are divided as (1) the exchangeable, (2) sorbed by amorphous glass and organic matter, (3) sorbed by oxide of Fe/Mn/Al, and (4) internal within the sorbent crystal structure. Differentiation of these four fractions was achieved through sequential extraction, which was performed with zeolite/fly ash solids of LB-1, CHB-1 and LB5:CHB5-1 once they were Pb-saturated from leaching tests. The extraction results are listed in Table 6.1.

Table 6.1 Extraction results and mass balance computation

		CHB-1	LB-1	LB5:CHB5-1	LB5:CHB5-3
Fraction (%)	Exchangeable	11%	5%	7%	11%
	Glass sorbed	17%	69%	32%	9%
	Mn/Fe oxide sorbed	39%	25%	35%	45%
	Internal	33%	1%	26%	35%
Total Pb^{2+} extracted (mg/g)		192.6	49.7	148.6	119.8
Total Pb^{2+} by Eq. (6.13) (mg/g)		216.7	54.0	183.1	154.8
Extraction error		-11.1%	-7.9%	-18.9%	-22.6%

The total Pb^{2+} extracted from one specimen is compared with the total Pb^{2+}

computed from Eq.(6.13) for the same specimen. The extraction value for CHB-1, LB-1, and LB5:CHB5-1 is 11.1%, 7.9%, or 18.9% smaller than the respective value of the actual Pb^{2+} sorption. The underestimation of the sorbed Pb^{2+} by the extraction results from analytical error and mainly the incomplete release of Pb^{2+} associated with some or all the reactant agents used in the four extraction steps. In spite of its shortcoming, the extraction protocol can still provide a semi-quantitative assessment of the relative role of different solid constituents in Pb^{2+} retention (Yong et al., 1992).

Figure 6.8(a) shows that, for CHB-1, oxides of Mn, Fe, and Al are the most preferential sorption sites that accommodate 39% of the total uptake of Pb^{2+}, followed by internal sites (33%), sites on amorphous glass (17%), and exchangeable sites (11%). Amorphous glass and oxides of Mn/Fe/Al combine to lend more than half of the Pb^{2+} retention in the forms of Pb-complex and Pb-precipitation. Sorption on internal sites reflects the ionic sieving property of CHB. The effective exchanging capacity of CHB only accounts for one tenth of the total sorption. This suggests that the sorption capacity of CHB should be evaluated not only by CEC but also in other specific forms

Unlike in Figure 6.8(a), Pb^{2+} fixed on LB-1 (Figure 6.8(c)) mainly belongs to the fraction of amorphous glass and organic matter. The organic matter in LBash appears as unburnt carbon that bears carboxyl groups (-COOH). The surface functional groups immobilize Pb^{2+} ions in stable chelates. The glass and organic fraction represents 69% of Pb^{2+} retention, exceeding the summation of the remaining three fractions. Oxides of Mn, Fe, and Al remain an important fraction responsible for one quarter of the total Pb^{2+} retention. Exchangeable sites rank the third among the four fractions with a 5% share of

the total Pb^{2+} removed. The internal sites seem a negligible fraction with only 1% of the Pb^{2+} retention, compared with the internal counterpart of CHB-1 that retained one third of its total Pb^{2+}. This striking difference is explained by the abundant interconnecting cavities within chabazite mineral.

In Figure 6.8(b), as might be expected, the partition of Pb^{2+} sorbed on LB5:CHB5-1 lies between the Pb^{2+} partitions for CHB-1 and LB-1. The significance of the four fractions in Pb^{2+} sorption ranks as Mn/Fe/Al oxides (35%) > glass and organic sites (32%) > internal sites (26%) > exchangeable sites (7%). Pb^{2+} ions sorbed on a mixture specimen, like LB5:CHB5-1, are mostly non-exchangeable. The internally sorbed Pb^{2+} is particularly stable, making the mixture material more compatible with subsurface environment.

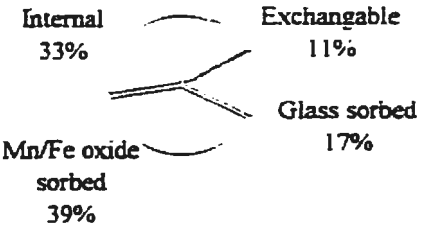

(Total Pb^{2-} sorbed = 216.7 mg/g solid)

(a) CHB-1

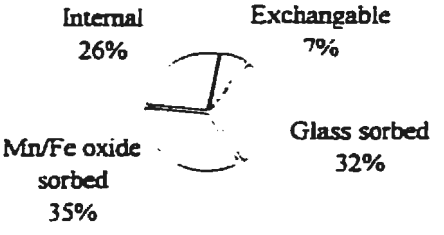

(Total Pb^{2-} sorbed = 183.1 mg/g solid)

(b) LB5:CHB5-1

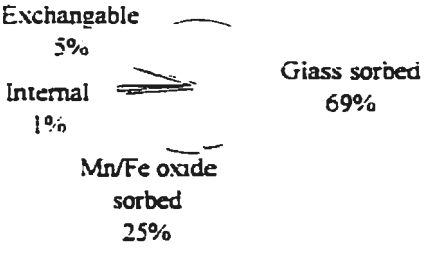

(Total Pb^{2-} sorbed = 54.0 mg/g solid)

(c) LB-1

Figure 6.8 Partition of Pb^{2-} sorption from leachate-1

6.3 Phenol Sorption

When leachate-2 was percolated into specimens of pure ash, pure zeolite, and their mixes, four typical reactions were involved in phenol sorption, i.e. (1) acid-base reaction; (2) dipole attraction; (3) intermolecular attraction; and (4) molecular sieving.

6.3.1 Acid-Base Reaction

The most characteristic nature of phenol (C_6H_5OH) is its acidity due to proton transfer from phenol to water molecules, i.e.

$$C_6H_5OH + H_2O \Leftrightarrow H_3O^+ + C_6H_5O^- \qquad (6.14)$$

The acid strength is defined by the acid ionization constant K_a,

$$K_a = \frac{[H_3O^+]\ [C_6H_5O^-]}{[C_6H_5OH]} \qquad (6.15)$$

With a pK_a (i.e. -log K_a) of 10 at 20°C, phenol is a stronger acid than alcohols, but a weaker acid than carboxylic acids.

In the leaching test using leachate-2, acid-base reaction took place readily between phenol and NaOH, KOH, $Ca(OH)_2$, $Mg(OH)_2$, which are the hydrolysis products of fly ash and zeolite. Phenol is converted quantitatively to phenoxides, i.e.

$$C_6H_5OH + NaOH \Leftrightarrow NaC_6H_5O + H_2O \qquad (6.16a)$$

$$C_6H_5OH + KOH \Leftrightarrow KC_6H_5O + H_2O \qquad (6.16b)$$

$$2C_6H_5OH + Ca(OH)_2 \Leftrightarrow Ca(C_6H_5O)_2 + 2H_2O \qquad (6.16c)$$

$$2C_6H_5OH + Mg(OH)_2 \Leftrightarrow Mg(C_6H_5O)_2 + 2H_2O \qquad (6.16d)$$

The reaction equilibria depend on pH. In case of extremely basic condition (e.g. pH = 13 or 0.1 N NaOH), 99.9% phenol would be converted to phenoxide (Gutsche and

Pasto, 1975). This, however, was not expected in the leaching tests of fly ash and zeolite, because the measured pH never reached such a high value. In the early stage of the leaching test on LB5:CHB5-2 (see Figure 5.7), the basicity of the specimen pore liquid was close to pH 10, at which phenol could be 50% in the phenol form (C_6H_5OH) and 50% in the phenoxide form ($C_6H_5O^-$) (Gutsche and Pasto, 1975). As the leaching test proceeded and the pH decreased, reactions of Eq. (16.6) were slowed down, and less and less phenol was converted to phenoxide, or more and more phenol migrated into effluent. Phenoxides need to be investigated further regarding their environmental toxicity.

6.3.2 Dipole Attraction

For a phenol molecule, oxygen in the -OH is considerably more electronegative than either carbon or hydrogen, and it permanently polarizes the molecule in the fashion shown in Figure 6.9. Because of this polar nature, phenol molecules are attracted onto oxide surface of fly ash and zeolite via the electrostatic force between opposite charges.

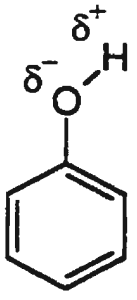

Figure 6.9 Polarity of a phenol molecule

(The δ^+ and δ^- represent fractional positive and negative charges, respectively)

The likelihood of electrostatic attraction between phenoxide ions ($C_6H_5O^-$) and certain positive charges on oxide surface is a function of the system pH. No such interaction is likely if the pH is higher than the "zero point of charge" (ZPC, i.e. the pH at which the solid surface charges from all sources are zero). Only when the pH is lower than the ZPC of the solid surface, i.e. when the surface concentration of H^+ is relatively high, can the oxide take on positive surface charges and act as an anion exchanger to attract $C_6H_5O^-$ ions.

The carboxyl group (-COOH) on the LBash surface has a charge-separated structure involving the polarization of the C=O bond and the nonbonded electron on the hydroxyl oxygen, as illustrated in Figure 6.10.

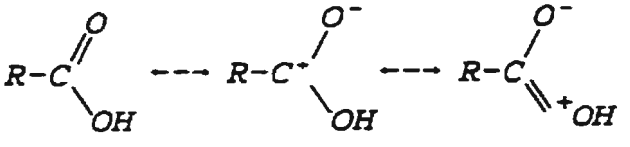

Figure 6.10 Representation of carboxyl group (R refers to a carbon framework)

The charge separated structure of the functional group gives rise to the organophillic property toward organic polar molecules. Therefore, phenol can be sorbed on the ash surface by orientation of unlike charges.

6.3.3 Intermolecular Attraction

During the early stage of phenol percolation in the leaching tests, as discussed

above, phenol molecules were sorbed on fly ash and zeolite mainly through dipole attraction. However, the retention in this stage might not be very significant because only a mono-layer coverage of phenol was formed on the solid surface, corresponding to the early-stage low sorption of the S shaped sorption isotherms in Figure 5.2. Following this stage, additional retention was created by the attraction between sorbed and non-sorbed phenol molecules. The intermolecular attraction operated as the result of an O-H---O interaction, which is referred to as a hydrogen bond and arises entirely from the -OH portion of phenol (as shown in Figure 6.11). Although it is less than 10% as strong as most covalent bonds, hydrogen bond is still strong enough to hold phenol molecules together. Consequently, phenol molecules on the surface mono-layer attract phenol from bulk pore solution, resulting in vertical alignment of the molecules on fly ash and zeolite surface. This phenomenon indicates the cooperative nature of sorption(Giles, et al.,1960), and hence explains the quicker rise in the intermediate stage of the S-type sorption isotherms in Figure 5.2.

6.3.4 Molecular Sieving

For zeolite, sorption sites are located on both external surface area (associated with macro-pores) and internal surface area (associated with micro-pores) of the crystals. The external sites are available for sorption of molecules of a broad range of sizes, whereas, the internal sites are available only to molecules small enough to enter the specific and uniform pores. Clearly, phenol has molecule size of 6.2Å that exceeds the micro-pore size of CHB (3.7×4.2Å), and will be excluded from molecular sieving. The sorbate can

merely be sorbed externally to macro-pores to a limited extent, because the external area is usually about one percent of the total surface area for typical zeolites (UOP Canada Inc., 1995). Thus, fly ash/zeolite mixes must rely on the ash content (i.e. LBash) to handle organic leachate (i.e. phenol).

6.3.5 CHB/LBash Ratio versus Phenol Retention

From phenol breakthrough curves of specimen LB-2, LB3:CHB7-2, LB5:CHB5-2, LB7:CHB3-2, and CHB-2, the sorption capacity of each test specimen with phenol from leachate-2 can be determined using computation similar to Eq.(6.13). The relationship between CHB/LBash ratio of a mixed specimen and the amount of phenol retained is plotted in Figure 6.12. The dependence of phenol sorption on LBash content is evident due to the affinity of phenol with unburnt carbon. The more LBash contained in a mixed specimen, the more phenol the specimen will retain. A pure LBash specimen is most effective as far as leachate-2 (i.e. phenol) is concerned.

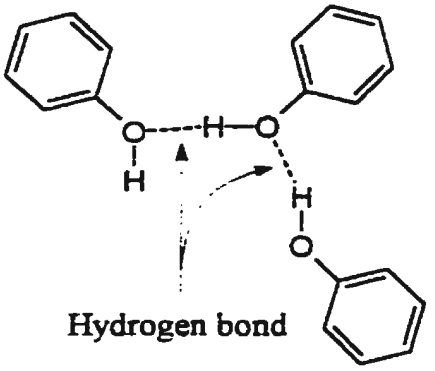

Figure 6.11 Hydrogen bonding interaction

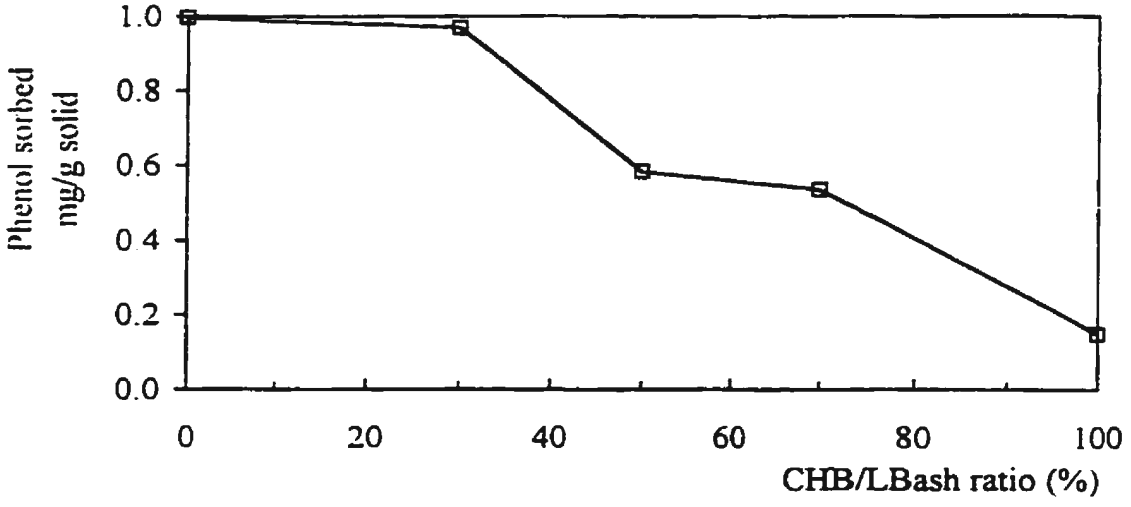

Figure 6.12 Phenol sorption versus CHB/LBash ratio

6.4 Effect of Phenol on Pb^{2+} Sorption

Although it is still a simplified formulation of a real MSW leachate, leachate-3 synthesized with Pb^{2+} (2500 ppm) and phenol (55 ppm) is a better simulation of the leachate chemistry encountered in a landfill site. During the leaching test of LB5:CHB5-3 using leachate-3, there was a depression of the Pb^{2+} sorption capacity. This inhibition is due to Pb^{2+} mobilization caused by Pb^{2+}-phenol complexes and the competition of phenol for sorption sites.

6.4.1 Pb^{2+} Complexation with Phenol

In an aqueous solution, as mentioned in Section 6.3.1, phenol is partly ionized into phenoxide ions ($C_6H_5O^-$) that serve as ligands to form complexes with Pb^{2+} ions when present, i.e.

$$n \cdot C_6H_5OH + Pb^{2+} + n \cdot H_2O \Leftrightarrow n \cdot (C_6H_5O)Pb^{2-n} + n \cdot H_3O^+ \qquad (6.17)$$

The complexation enhances phenol ionization and increases H^+ concentration, leading to a measurable drop of pH. To confirm the reaction in Eq. (6.17), a quick test was performed here by mixing 100 ml phenol solution (55 ppm and pH 6.5) with 100 ml Pb^{2+} solution (2500 ppm and pH 5.3). The resulting pH measured was 4.7, dropping below the two original pH values and suggesting the net release of H^+ from complexation. In addition, the polar molecules of phenol may function as ligands to directly form complexes with Pb^{2+}, without perturbing the system pH. Differentiation between free Pb^{2+} and complexed Pb^{2+} is useful although it is not always an easy task. Differential pulse anodic stripping voltammetry (DPASV) (Jin, 1996) was employed here to analyze an

aqueous solution which contained merely Pb^{2+} (40 ppb) and phenol (55 ppm) with pH 6.0. It was observed that, in this specific system, 25% of the Pb^{2+} was present as complexes and 75% as free ions. In more complex situations, as with LB5:CHB5-3, the distribution of Pb^{2+} between free and complexed forms must be a function of (1) the concentrations of complexing ligands (e.g. -OH, $C_6H_5O^-$, $-COO^-$), (2) the equilibrium constants for all the complexation reactions, (3) the pH, and (4) the total concentration of Pb^{2+} itself. Complexes formed with C_6H_5OH, $C_6H_5O^-$, as well as other ligands (e.g. -OH, and $-COO^-$) make Pb^{2+} ions more soluble in bulk solution, thus reducing their sorption onto the solids of LB5:CHB5-3.

6.4.2 Partition of Pb^{2+} Sorption Subject to Phenol Interaction

The total Pb^{2+} retention on LB5:CHB5-3, when it was Pb^{2+} saturated, was determined from its breakthrough curve (Figure 5.10) using Eq. (6.13). The partition of the total Pb^{2+} among the previously defined four fractions was estimated through sequential extraction. The result of the extraction is compared with the extraction data from LB5:CHB5-1 in Figure 6.13. The specimen LB5:CHB5-1 and LB5:CHB5-3 had the same solid composition and same exposure to Pb^{2+} percolation, but LB5:CHB5-3 was also subject to phenol interaction as opposed to LB5:CHB5-1. Figure 6.13 shows that the total Pb^{2+} retention on LB5:CHB5-3 (154.8 mg/g solid) is 84.5 % as much as the total Pb^{2+} retention on LB5:CHB5-1 (183.1 mg/g solid). The percentage of Pb^{2+} sorbed on glass and organic sites reduced to 9% with LB5:CHB5-3 as compared to 32% on the corresponding sites with LB5:CHB5-1. This is because the unburnt carbon in LBash preferentially

attracted phenol molecules rather than Pb^{2+} ions. Proportionally, the percentage of Pb^{2+} sorbed in the other three fractions were more or less increased, while the exact impact of phenol on Pb^{2+} precipitation, Pb^{2+} complexation, and Pb^{2+} exchanging can hardly be appreciated. Nevertheless, since the zeolite micro-pores are beyond the reach of phenol molecules, the actual amount of Pb^{2+} sorbed on internal sites is not expected to be significantly altered.

Hence, when Pb^{2+} and phenol percolate simultaneously a CHB-LBash mixture specimen, phenol molecules mainly occupy the organophillic sites on LBash solids, but the internal sorption sites within CHB crystals are always reserved for Pb^{2+} ions. In terms of overall retention, the mixture material remains compatible with the two individual leachate constituents.

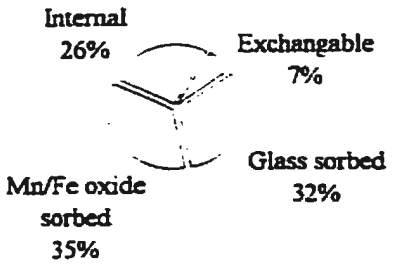

(Total Pb^{2-} sorbed =183.1 mg/g solid)

(a) LB5:CHB5-1

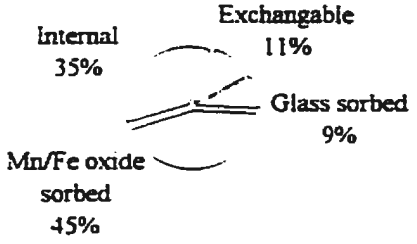

(Total Pb^{2-} sorbed =154.8 mg/g solid)

(b) LB5:CHB5-3

Figure 6.13 Partition of Pb^{2-} sorption from leachate-1 and leachate-3

6.5 Optimum CHB-LBash Mix

It becomes clear from the experimental results and the relevant discussion that mixes of CHB and LBash are capable of effectively retaining Pb^{2+} ions and phenol molecules from leachate. CHB is the principal sorbent to fix Pb^{2+} on its various and plentiful sorption sites. The internal micro-pores within CHB crystals possess a sieving selectivity to trap Pb^{2+} ions very stably. The more CHB contained in a mix, the more Pb^{2+} the composite material can retain (Figure 6.7). On the other hand, the LBash content in a mixture is mainly responsible for phenol sorption. The unburnt carbon on LBash solids attracts phenol molecules selectively. Increasing LBash content in a mixture readily enhances phenol sorption (Figure 6.12).

To give equal attentions to organic and inorganic leachates, the CHB/LBash ratio should be set appropriately. The hydraulic performance of a proposed composite material also needs to be taken into account. After careful inspection of the relationship between CHB content and Pb^{2+} sorption (Figure 6.7), the relationship between LBash content and phenol sorption (Figure 6.12), and the relationship between CHB/LBash ratio and the hydraulic conductivity of a compacted mixture specimen (Figure 6.1), a compromise can be made at 1:1 of CHB/LBash ratio. This is the optimum ratio of CHB-LBash mixes under present experimental conditions. At this ratio, the mixture specimen exhibits effective retentions with Pb^{2+} and phenol, and minimum hydraulic conductivity of 3.0×10^{-9} m/s.

7 CONCLUSIONS

7.1 Summary and Conclusions

Based on the results of this study, the following conclusions can be drawn:

(1) LBash represents a high-carbon fly ash, which is distinguished from NSash by its unburnt carbon content, particle morphology, and surface functional groups.

(2) CHB represents chabazite, one of the principal natural zeolites. Compared to CLN (clinoptilolite), it has a lower Si/Al ratio, higher grade of zeolite purity, higher chemical activity, and larger cation exchange capacity.

(3) The hydraulic conductivity of CHB with Pb^{2+} permeant is slightly lower than that for LBash. CHB-LBash mixes become even more impermeable due to better filling of pore space. No significant alteration of hydraulic conductivity was observed when different permeants were used.

(4) CHB is the most powerful among CHB, CLN, LBash, and NSash in Pb^{2+} sorption. It sorbs up to 210 mg Pb^{2+} per gram of dry solid under the batch test conditions.

(5) LBash is more effective than the remaining three candidate materials in phenol removal, which ideally amounts to 1.3 mg phenol per gram of dry solid.

(6) The CHB-LBash mixes show significant basicity due to the hydrolysis of fly ash and zeolite (pH>7). The pH strongly influences the interaction between the mixture solids, Pb^{2+}, and/or phenol.

(7) Pb^{2+} sorption takes place on LBash and CHB solids through physisorption, chemisorption, complexation, precipitation, and ionic sieving of CHB micro-pores.

(8) When merely Pb^{2+} ions percolate into pure CHB material, the partitioning of total

Pb^{2+} sorbed on different sorption sites ranks as *Mn/Fe/Al oxide* (39%) > *internal* (33%) > *amorphous glass* (17%) > *exchangeable* (11%). When the same percolation is applied to pure LBash material, the partitioning of total Pb^{2+} sorption ranks as *glass and organic matter* (69%) > *Mn/Fe/Al oxide* (25%) > *exchangeable* (5%) > *internal* (1%).

(9) Phenol leachate is attenuated in LBash and CHB matrix via acid-base reaction, dipole attraction, and hydrogen bonding. Molecular sieving property of CHB does not favour the removal of phenol, because phenol molecule is too big in size to fit into CHB micro-pores.

(10) when a CHB-LBash mix is leached with Pb^{2+} and phenol simultaneously, the two leachates compete for all sorption sites except for the CHB micro-pores, which cannot accommodate the size of phenol molecules.

(11) Mixture specimens are suitable for retaining combined leachates. CHB is the principal sorbent with Pb^{2+}, while LBash is mainly responsible for phenol attenuation.

(12) Under present experimental conditions, a CHB/LBash ratio of 1:1 appears to be the optimum composition for a liner material which will exhibit a maximum overall retardation of Pb^{2+} and phenol. The 1:1 mixture compacted under standard conditions also shows a minimum hydraulic conductivity in the order of 3.0×10^{-9} m/s.

7.2 Suggestions for Further Research

The study of composite materials for environmental applications is almost unlimited. It is however recommended that the zeolite/fly ash mixes be examined in more detail by:

(1) adding new heavy metal ions (e.g. Cr^{3+}, Cd^{2+}, Cu^{2+}, etc.) into the synthetic leachate to evaluate the overall sorption capacity;

(2) testing the affinity of the mixes for organic compounds of different molecule sizes;

(3) investigating the influence of pH on the retention properties of the zeolite/ash mixes;

(4) improving the hydraulic and mechanical properties of the composite material by addition of impervious clays.

REFERENCES

ASTM. 1996a. Standard test method for particle size analysis of soils (D422-63). *In* 1996 Annual book of ASTM standards, Sec. 8, Vol. 4, ASTM, Philadelphia, pp. 10-20.

ASTM. 1996b. Test method for laboratory compaction characteristics of soil using standard effort (D698-91). *In* 1996 Annual book of ASTM standards, Sec. 8, Vol. 4, ASTM, Philadelphia, pp. 75-82.

Ames, L.L. 1960. The cation sieve properties of clinoptilolite. American Mineralogy, **45**: 689-700.

Barrer, R.M., and Kerr, I.S. 1959. Intracrystalline channels in levynite and some related zeolites. Transactions Farady Society, **55**: 1915-1923.

Berry, E.E. 1978. Fly ash for use in concrete, part 2: A critical review of the effects of fly ash on the properties of concrete, Report 78-16, CANMET, Energy, Mines and Resources, Canada.

Bole, J.R. 1972. Composition, optical properties, cell dimensions, and thermal stability of some heulandite group zeolites. American Mineralogist, **57**: 1449-1462.

Bowders, J.J. 1988. Fly ash liners for waste disposal facilities. Geotechnical News, **6**(4): 26-29.

Breck, D.W. 1974. Zeolite molecular sieves. John Wiley & Sons, Inc., New York.

Brown, D.W., and Hem, J.D. 1984. Development of a model to predict the adsorption of lead from solution on a natural streambed sediment. U.S. Geological Survey

Water-Supply Paper, I19.13:2187.

Carter, M.R. 1993. Soil Sampling and Methods of Analysis. Canadian Society of Soil Science, Lewis Publishers, Boca Raton, Florida.

Chan, H.T. 1991. Compacted fly ash with additives: a potential construction material for hydraulic barriers. Ontario Hydro Research Division, Ontario Hydro, Toronto, Ont., Research report 91-98-K.

Chan, H.T. 1990. Coal ash -- a resource material. Ontario Hydro Research Division, Ontario Hydro, Toronto, Ont., Research report 89-288-K.

Cyr, F., Mehra, M.C., and Mallet, V.N. 1987. Leaching of chemical contaminants from a municipal landfill site, Bulletin of environmental contamination and toxicology **38**: 775-782.

Eaton, P.B., Gray, A.G., Johnson, P.W., and Hundert, E. 1993. State of the environment in the Atlantic region, Environment Canada, Atlantic region.

Edil, T.B., Sandstrom, L.K., and Berthouex, P.M. 1992. Interaction of inorganic leachate with compacted pozzolanic fly ash. J. of Geotechnical Engineering, **118**(9): 1410-1430.

Environment Canada, 1985, Phenol, environmental and technical information for problem spills. Environmental Protection Service, Ottawa, Ontario.

Evans, J.C., Sambasiva, Y., and Zarlinski, S.J. 1990. Attenuating materials in composite liners. *In* Waste containment systems: construction, regulation, & performance. ASCE Geotechnical Special Publication No.26, pp.246-263.

Folkes, D.J. 1982. Control of contaminant migration by the use of liners. Canadian Geotechnical Journal, **19**: 320-344.

Gasser, U.G., Walker, W.J., Dahlgren, R.A., Rorch, R.S., and Burau, R.G. 1996. Lead release from smelter and mine waste impacted materials under simulated gastric conditions and relation to speciation. Environmental Science & Technology, **30**: 761-769.

Giles, C.H., MacEwas, T.H., Nakwa, S.N., and Smith, D. 1960. Studies in adsorption. Part XI. A system of classification of solution adsorption isotherms, and its use in diagnosis of adsorption mechanisms and in measurement of specific surface ares of solids. Journal of Chemistry Society, 3973-3993.

Goldman, L.J., Greenfield, L.I., Damle, A.S., Kingsbury, G.L., Northeim, C.M., and Truesdale, R.S. 1990. Clay Liners for Waste Management Facilities, Design, Construction and Evaluation, Noyes Dada Corporation, New Jersey.

Government of Canada, 1991. The state of Canada's environment. Banfield-Seguin Ltd., Ottawa.

Gutsche, C.D., and Pasto, D.J. 1975, Fundamentals of Organic Chemistry, Prince-Hall, Inc, New Jersey.

Hammond, A. 1991. Environmental almanac. Houghton Mifflin Company, New York.

Harkins, D.B. 1984. Occurrence and availability of natural zeolites. *In* Zeo-Agriculture, use of natural zeolites in agriculture and aquaculture. *Edited by* W.G. Pond, and F.A. Mumpton, Westview Press/Boulder, Colorado, pp.69-78.

Heystee, R.J., Johnston, H.M., and Chen, H.T. 1991. Coal fly ash properties and ash

landfill design. Proceedings of the first Canadian conference on environmental geotechnics. *Edited by* R.P. Chapuis and M. Aubertin, the Canadian Geotechnical Society, pp.65-71.

Hwa, T.J. 1991. Leachate of fly ash derived from refuse incineration. Environmental assessment and monitoring, **19**: 157-164.

Jin, L. 1996. Differential pulse anodic stripping voltammetry (DPASV), Personal communication.

Joshi, V.M. and Malhotra, V.M. 1985. Relationship between pozzolanic activity and chemical and physical characteristics of selected Canadian fly ashes. *In* Fly ash and coal conversion by-products: characterization, utilization, and disposal II, Mat. Res. Soc. Symp. Proc. Vol. 65. *Edited by* G.J. McCarthy and R.J. Lauf, Materials Research Society, Pittsburgh, pp.167-170.

LaGrega, M.D., Buckingham, P.C., and Evans, J.C. 1994. Hazardous Waste Management. MaGraw-Hill, Inc., New York.

Matrecon, Inc. 1980. Lining of waste impoundment and disposal facilities. Municipal Environmental Research Laboratory, Office of Research and Development, USEPA, Report SW-870, Cincinnati, OH.

McCarthy, G.J. 1988. X-ray diffraction analysis of fly ash. Advances in X-ray analysis, **32**: 331-342.

Mercer, B.W., Ames, L.L. and Smith, P.W. 1970a. Cesium purification by zeolite ion exchange. Nucl. Appl. & Tech. **8**: 62-69.

Mercer, B.W., Ames, L.L., Touhill, C.J., Van Slyke, W.J. and Dean, R.B. 1970b.

Ammonia removal from secondary effluents by selective ion exchange. J. of Water Pollution Control Federation. 42: R95-R107.

Mitchell, J.K. 1993. Fundamentals of soil behavior. John Wiley & Sons Inc., New York.

Mitchell, J.K., Hooper, D.R., and Campanella, R.G. 1965. Permeability of compacted clay. ASCE Journal of the Soil Mechanics and Foundations Division, 91(SM4): 41-65.

Moell, C.E. 1977. Leachate and gas migration from the clover bar sanitary landfill site -- Edmonton, Environmental Protection Services, Alberta Environment, Edmonton, Alberta, Report 1184.

Morel, F.M., Westall, J.C., and Yeasted, J.G. 1981. Adsorption Models: a Mathematical Analysis in the framework of general equilibrium calculations. *In* Adsorption of Inorganics at Solid-liquid Interfaces. *Edited by* M.A. Anderson, and A.J. Rubin, Ann Arbor Science Publishers, Inc., pp. 263-294.

Mumpton, F.A. 1984. Natural Zeolite, *In* Zeo-Agriculture, Use of Natural Zeolites in Agriculture and Aquaculture. *Edited by* W.G. Pond, and F.A. Mumpton, Westview Press/Boulder, Colorado, pp.33-43.

Mumpton, F.A. 1960. Clinoptilolite redefined. American Mineralogist, 45: 351-369.

Nhan, C.T. 1994. A coal fly ash liner: an option in solid waste disposal management. M.a. Sc. Thesis, University of Toronto, Toronto, Ont.

Peirce, J.J. 1984. Effect of inorganic leachates on clay liner permeability. Final Report by Duke University, USEPA, EPA-68-03-3149, 24-1, Cincinnati, Ohio, 1984.

Rowe, R.K., and Hrapovic, L. 1996. HDPE geomembrane and diffusion. Proceedings of

49th Canadian Geotechnical Conference, St. John's, Nfld., September 23-25, 1996, Volume 2, pp. 623-629.

Roy, D.M., Luke, K. and Diamond, S. 1985. Characterization of fly ash and its reaction in concrete. *In* Fly ash and coal conversion by-products: characterization, utilization, and disposal I, Mat. Res. Soc. Symp. Proc., Vol. 43. *Edited by* G.J. McCarthy and R.J. Lauf, Materials Research Society, Pittsburgh, pp.3-20

Roy, W.R., Krapac, I.G., Chou, S.F.J., and Griffin, R.A. 1991. Batch-type procedures for estimating soil adsorption of chemicals. EPA/530-SW-87-006-F, USEPA.

Schindler, P.W. 1981. Surface complexes at oxide water interfaces. *In* Adsorption of Inorganics at Solid-liquid Interfaces. *Edited by* M.A. Anderson, and A.J. Rubin, Ann Arbor Science Publishers, Inc., pp. 1-50.

Scott, H.D., Wolf, D.C., and Lary, T.L. 1982. Apparent adsorption and microbial degradation of phenol by soil. J. of Environmental Quality, **11**: 107-111.

Singh, B.K., and Rawat, N.S. 1994. Comparative sorption kinetic studies of phenolic compounds on fly ash and impregnated fly ash. J. Chem. Tech. Biotechnol. **61**: 57-65.

Smith, J.V. 1962. Crystal structures with a chabazite framework, I. Dehydrated Ca-chabazite. Acta Crystallographica, **15**: 835-845.

UOP Molecular Sieves, 1995, UOP Canada Inc.

USEPA, 1977. The report to congress: waste disposal practices and their effects on ground water. Report No. EPA-570/9-77-002, Washington D.C.

Vesperman, K.D., Edil, T.B., and Berthouex, P.M. 1985. Permeability of fly ash and fly ash-sand mixtures. *In* Hydraulic Barriers in Soil and Rock, ASTM STP 874. *Edited by* A.I. Johnson, R.K. Frobel, N.J. Cavalli, and C.B. Pettersson, American Society for Testing and Materials, Philadelphia, pp.289-298.

Weast, R.C. 1975. Handbook of Chemistry and Physics. CRC Press Inc., Boca Raton.

Wright, D.R. 1980. Coal-fired power plants. Canadian mining and metallurgical bulletin, **73**: 124-142.

Yong, R.N., Mohamed, A.M.O., and Warkentin, B.P. 1992. Principles of Contaminant Transport in Soils. Elsevier Science Publishers, Amsterdam.